DoE/ID/12945--T3

Ion Sensitive Field Effect Transistors Applied to the Measurement of the pH of Brines

DOE/ID/12945--T3

DE93 005209

A Thesis

Presented to

The Graduate Faculty of

The University of Southwestern Louisiana

In Partial Fulfillment of the

Requirements for the Degree

Master of Science

FG07-90ID12945

Jie Chen

Summer 1991

Ion Sensitive Field Effect Transistors Applied to the Measurement of the pH of Brines

Jie Chen

Approved:

John R. Meriwether, Chairman
Professor of Physics

Dean F. Keeley
Professor of Chemistry

L. Dwynn Lafleur
Professor of Physics

Joan T. Cain
Dean, Graduate School

ACKNOWLEDGEMENTS

I would like to thank all of those people who helped me to complete my masters work while here at USL. Many thanks go out from the bottom of my heart to all of my committee members, Dr. John R. Meriwether, Dr. Dean F. Keeley and Dr. L. Dwynn Lafleur, other faculty members, and especially Mr. William K. Koon, without whom I would not have been able to complete my work.

Sincere appreciation is expressed to Dr. John R. Meriwether for his direction of my study and research as well as the preparation of this thesis.

TABLES OF CONTENTS

Pages

LIST OF TABLES

Pages

LIST FIGURES

Pages

CHAPTER 1. INTRODUCTION

§1.1. The Purpose of the Research

The ability to measure the pH (the negative logarithm of the hydrogen ion activity) of harsh fluids such as geothermal oil field brines is important, since pH is a fundamental property; as one chemist stated: "very often pH is a critical test because its accuracy lays the foundation for other measurements" [1]. In our research, we focus on the analysis of brines similar to those found in underground geothermal reservoirs. Since the brines are deep under the ground, the values of the pressure and the temperature are high (up to 14 MPa and 150°C); therefore the usual methods of pH measurement, e.g., glass electrode, are not applicable. The hydrogen ion sensitive ISFET (Ion Selective Field Effect Transistor) was studied as a pH sensor in this research. An ISFET can detect the electrochemical potential difference between the solution and the semiconductor due to the concentration of H^+ ions in the solution. Because of its solid state construction, an ISFET should work properly under high pressure and high temperature conditions. Earlier results [2], [3], [4], have indicated that it is possible to use ISFETs under the harsh conditions presented by geothermal brines.

§1.2. Historical Review of the Development of the ISFET

From the historical perspective, electrical engineers and solid state physicists are the pioneers of the field of the CSSD (chemically sensitive semiconductor device). Later, electro-analytical chemists and bioengineers joined in and contributed to the development of this area. There are certain

advantages which are inherent in solid state chemical sensors: they respond rapidly, have small size, and because of their solid state fabrication, they are very stable.

The ISFET is a kind of CHEMFET (Chemically Sensitive Field Effect Transistor) which belongs to the family of CSSDs. The first report on the CHEMFET can be traced back to 1970 when Bergveld published his short communication [5]. One year later, Matsuo, Esashi, and Iinuma [6]. reported a similar device. In 1972, Bergveld [7] published the first full description of an ISFET sensitive to hydrogen and sodium ions, in which he stated, "The device makes it possible to measure ion activities without using a reference electrode." He used the device for measurement of pH and sodium ion activity and for recording physiological transient action potentials. He also presented the electronic circuit and detailed results of the measurement of Na^+ and H^+ ion activities. Matsuo and Wise described another pH-sensitive ISFET in 1974 [8], which basically is an n-channel depletion mode MOSFET (Metal-Oxide Field Effect Transistor). Their paper reported the preliminary data on a field-offset structure which was used for recording and monitoring ion concentrations. In Matsuo's device, there were two layers, one was thermally grown SiO_2 and the other was pyrolytically deposited Si_3N_4, while in Bergveld's device there was only one thermally grown SiO_2 layer. The existence of pinholes in the SiO_2 layer caused a degradation of its insulating properties [9] and further made it difficult to formulate a coherent model of operation of these devices. The difference between Matsuo's and Bergveld's models caused a significant discussion which was important in the development of these devices. Bergveld did not use an external reference electrode, and he claimed the reference electrode was not needed for the operation of an ISFET

[7]. It was proved theoretically and generally accepted later that the external electrode reference is required for proper operation of a CHEMFET. Other reports describing pH, pK, pNa and pCa ISFETs [4] have appeared.

Zemel wrote the first review of chemically sensitive semiconductor devices [10] in 1975. He addressed the principles of the operation and relationships of MOSFETs, CSSD, ISFETs, Heterojunction and Schottky Barrier Structures. Another review focusing on ISFETs was written by Janata and Moss [11] in 1975. In this article, they presented the theory of operation and the structure of a potassium sensitive field effect transistor, and compared its performance with the corresponding conventional PVC-type ion selective electrodes. They characterized the FET's performance as a solid state field effect device and as an electrochemical sensor. They stated: "The transistor operates satisfactorily in the presence of proteins and it has been used for determination of potassium ion concentration in blood serum.". In 1977, Revesz [12] presented another paper which dealt particularly with the role of the surface states in the mechanism of the operation of ISFET. A theoretical analysis of the solution/membrane/insulator/semiconductor structure, supplemented by a thorough experimental study of the system, was published by Buck and Hackleman [13]. The promising features of CHEMFETs have attracted many scientists and research groups to the field, e.g., J. N. Zemel, J. Janata and R. P. Buck in the USA., P. Bergveld in the Netherlands, T. Matsuo and T. Akiyama in Japan, A. Sibbald in England, Yu. G. Vlasov in the USSR., K. Nagy and T. A. Fjeldy in Norway.

In 1984, Morf, Oggenfuss, and Simon [14] reported a "unified approach to the theory of ion-selective liquid membrane electrodes". In their paper, the

potential response and selectivity behavior towards monovalent cations and anions was described for membranes containing different ion-exchange sites and neutral carriers. In the same year, Janata gave a lecture [15] on the application of CHEMFETs in analytical and physical chemistry, and reviewed the technology of the preparation of CHEMFETs. At that time the average lifetimes of membrane-based ISFETs had exceeded sixty days. Later, in 1987, Van Der Schoot and Bergveld [16] in a short communication on the pH-Static Enzyme Sensor, reported an ISFET-based urea sensor combined with a noble-metal electrode which provided for continuous coulometric titration of an enzymatic reaction. In 1989, Alean Kirkpatrick and Hertz [2] published a paper which described a method for in-situ pH monitoring of rainfall and the compensation for the effect of temperature. In 1990, Knauss, Wolery, and Jackson [3] published a letter which proposed an operational and theoretical approach to dealing with pH in brines and other concentrated aqueous solutions. They used several different ion selective electrodes corresponding to different types of ions. The potential measured was proportional to pHCl = pH + pCl or pH/Na = pH – pNa depending on the type of the other electrodes. Then they used the Pitzer equation to compute a thermodynamic model of the solution, as they stated "A pH scale convention is then used to decouple pH from pCl, pNa, pBr, etc.". The direct coupling of chemical and electric fields in the gate opens new classes of sensors. Thus, changes in electron work function can be analytically utilized and the work function of various materials can be directly measured.

Recently, other applications have been made in biomedical science [17], [18], geological science [3], [4], chemical engineering, physical chemistry [15] and many other fields. As the technology improved [1], [19], [20], [21],

[22] more sophisticated probes have been designed for more specific tasks. The progress of the materials selection and deposition technique of ion-selective membranes [14], [20] has improved the stability and ion selectivity, and further expanded the applications of ISFETs. The desire for in-line monitoring of the ion concentrations and development of multi-species probes [17], [18], [23] appears to be the trend in the development of ISFETs. Durability, fast response time, and small size are the advantages that the ISFET brings to these problems.

§1.3. The Research

In our research, we used ISFETs in NaCl solutions of varying pH values and measured the ISFET output signal which was amplified by a linear amplifier. A heated pressure cell was designed and built to simulate the high temperature and high pressure conditions found in the geothermal brines. The pressure cell can generate a pressure more than 176 MPa and the heater can heat the sample to over 240 °C. We have measured the pH of brine solution as a function of pressure to 40 MPa and temperature to 70°C.

CHAPTER 2. ISFET

§2.1. The Structure of ISFET

The structure of an ISFET is shown in Figure 2.1. It is an n-channel depletion mode FET. A conducting channel is formed by the interface of a semiconductor and an insulator on the semiconductor side in response to ions passing through the membrane. The source region is the electron supplier and the electrons drain from the drain region. It is the membrane covering the ISFET which provides the device its ionic selectivity.

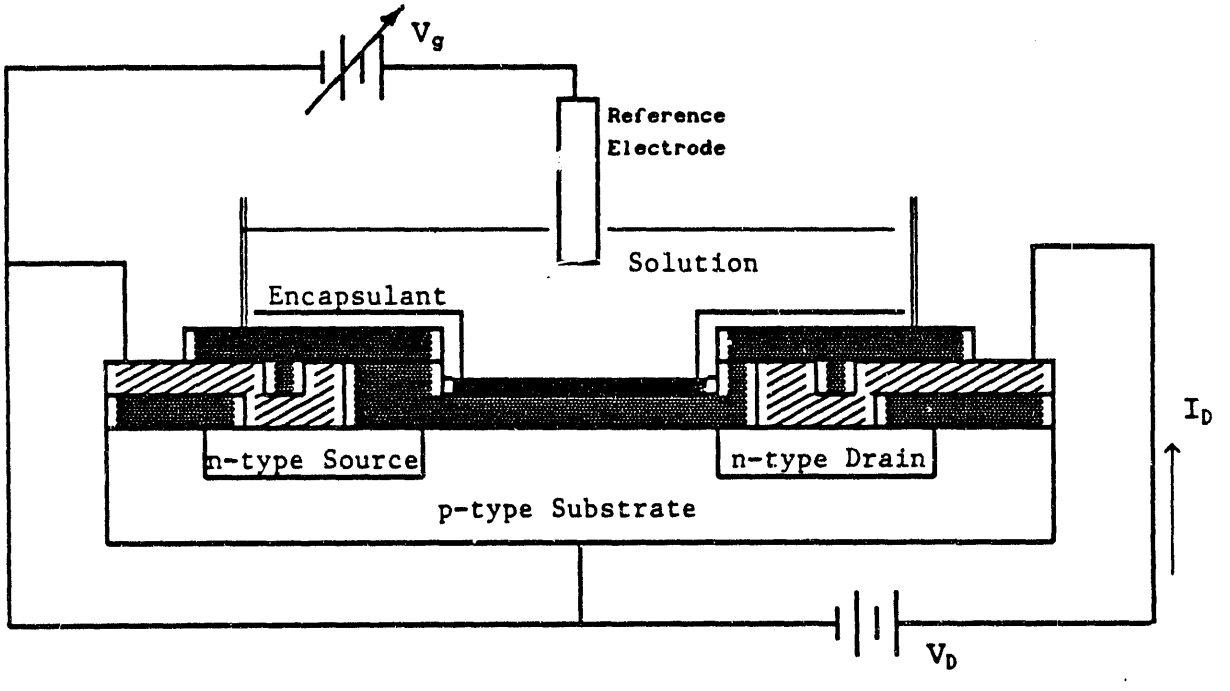

Figure 2.1 ISFET. ▮ , insulator; ▒ , metal; ▮ , membrane

The structure of an ISFET is

metal (external electrode reference)/membrane/insulator/semiconductor.

It can be simplified to a metal/insulator/semiconductor (MIS) structure, the

most basic structure of IGFETs (Insulated Gate Field Effect Transistor). The purpose of this chapter is to discuss the MIS structure then extend it to IGFETs and finally to include ISFETs.

1. The Ideal MIS Structure

Figure 2.2 shows the MIS structure. The characteristics of the ideal MIS structure is defined as:

(1) The electron work functions W_m of the metal and W_s of the semiconductor are equal, i.e., $W_{ms} = W_m - W_s = 0$.

(2) The insulator is a perfect insulator, thus, there is no charge distribution in the insulator and no charge transport through the insulator.

(3) There are no surface states for semiconductor, i.e., the ideal semiconductor band structure extends to the surface.

For the ideal MIS structure, when no voltage is applied on the gate (V_g = 0), the energy band structure of the semiconductor is flat, as shown in Figure 2.3. But if $V_g \neq 0$, the band structure of the semiconductor will be bent, and the Fermi levels of metal and semiconductor separated by qV_g, as shown in Figure 2.4.

There are three biasing conditions ($V_g < 0$, $V_g > 0$, and $V_g >> 0$) which are described below (We consider the p-type semiconductor here; the n-channel FET will be discussed later).

(1). **Accumulation:** For $V_g < 0$, additional holes are attracted to the semiconductor-insulator interface on the semiconductor side. The semiconductor behaves like a conductor.

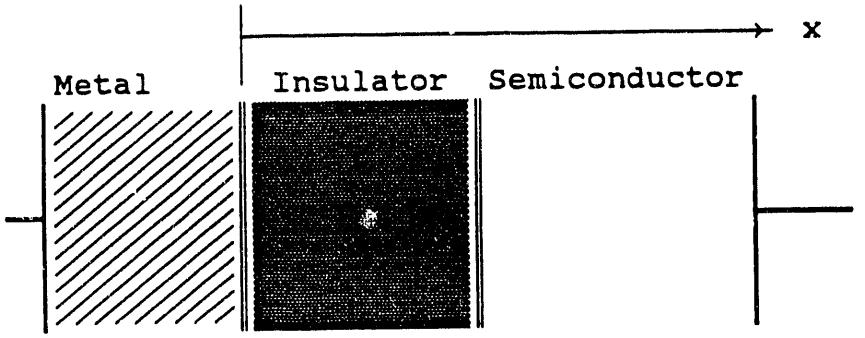

Figure 2.2 MIS Structure

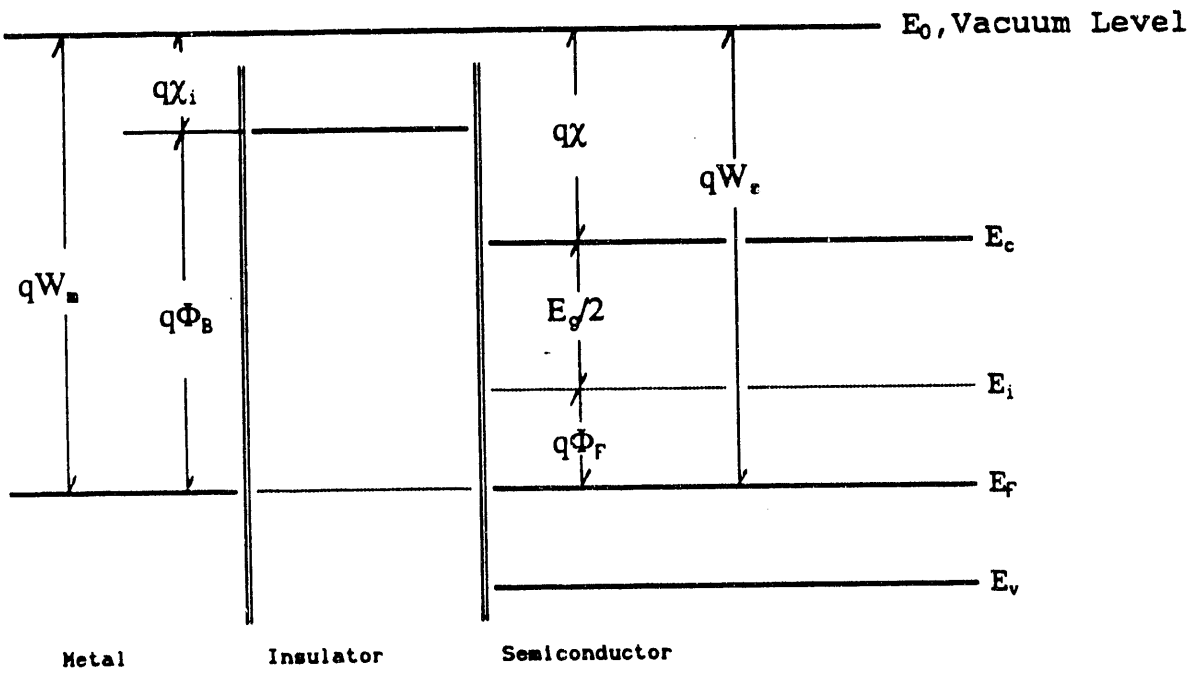

Figure 2.3 Energy Band Diagram of an MIS Structure for p-type Semiconductor q, the electron charge; W_m, the metal work function; W_s, the semiconductor work function; Φ_B, the barrier potential; Φ_F, Fermi potential; E_g, band-gap energy; χ, electron affinity of the semiconductor; χ_i, insulator electron affinity; E_c, semiconductor's conducting band; E_i, semiconductor's intrinsic band; E_v, semiconductor's valence band

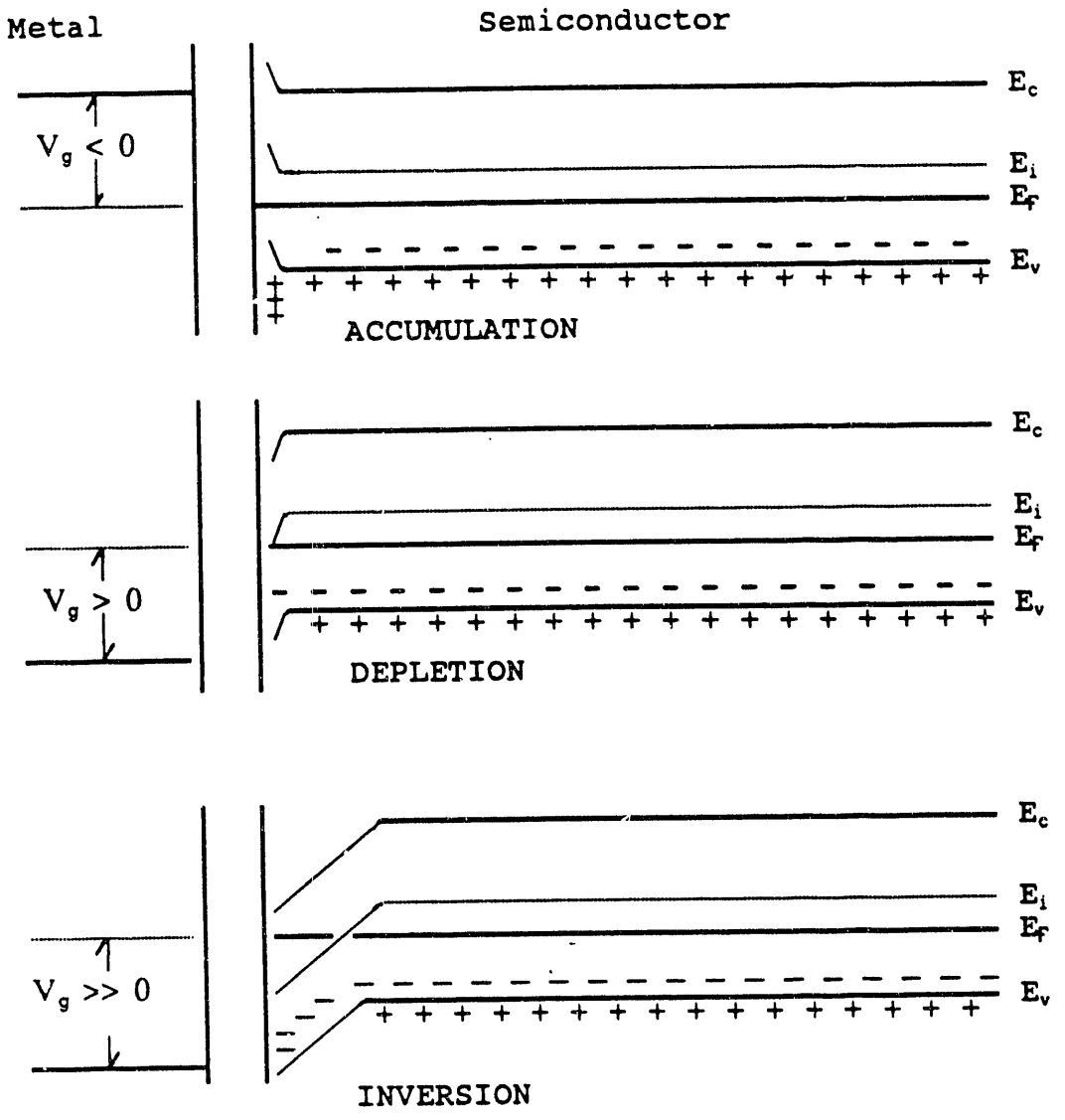

Figure 2.4 The Energy Band Diagrams of an MIS Structure with p-type Semiconductor Different Biasing Conditions

(2). **Depletion:** For $V_g > 0$, holes are repelled from the semiconductor-insulator interface and immobile negative charge accepter atoms are left. Thus the semiconductor behaves much like an insulator. According to electrostatic theory, the energy bands of the semiconductor shift up, as shown in Figure

2.4.

(3). **Inversion:** For $V_g >> 0$, when V_g is sufficiently large, the energy bands of the semiconductor will be bent so much that the intrinsic level, E_i, will cross the Fermi level, E_F. That means $E_F - E_i > 0$ near the insulator. In general, the hole density, ρ_h, and the electron density, ρ_e, depend exponentially on the value of $\pm(E_i - E_F)$, that is,

$$\rho_h \propto \exp[(E_i - E_F)/2KT] \text{ , and}$$
$$\rho_e \propto \exp[(E_F - E_i)/2KT].$$

When $E_F - E_i > 0$, the electron density is so great that ρ_e will exceed ρ_h near the semiconductor insulator interface. The band displacement, $E_F - E_i$, reaches its maximum value, $q\Phi_F$, at the interface. Here q is the charge of the electron and Φ_F is the Fermi potential. Thus, a conducting 'electron layer' exists on the semiconductor side of the semiconductor-insulator interface. Now, the p-type semiconductor behaves like a n-type semiconductor. This is called "semiconductor inversion". When the band displacement reaches $2\Phi_F$ the condition is called the 'strong inversion'. The voltage V_g producing strong inversion is called the 'threshold voltage', labeled V_T. This is an important parameter because under strong inversion, the band displacement of the semiconductor reaches its maximum value. When $V_g > V_T$, the electron density at the semiconductor-insulator interface increases as V_g increases but the band displacement will not. This inversion biasing condition is emphasized because the FET works under this condition.

For the ideal MIS structure, V_T is given as $$V_T = -\frac{Q_B}{C_0} + 2\Phi_F, \qquad (1)$$

where Q_B is the surface charge density of the charge region and C_0 is the capacitance per unit area of the capacitor formed by the metal and semiconductor in the MIS structure.

2. The Threshold Voltage of Non-Ideal MIS Structure

In the non-ideal MIS structure, there are three non-ideal effects which must be considered:

(1) $W_{ms} = W_m - W_s \neq 0$, i.e., there is a work function difference between metal and semiconductor. It means there is a charge flow that exists between metal and semiconductor. (2) Since the insulator is non-ideal, there is a charge distribution of density $\rho'(x)$ in the insulator which induces an image charge distribution in both metal and semiconductor. (3) There is a dense positive charge layer, Q_{ss}, at the insulator side of the insulator-semiconductor interface. This Q_{ss} is due to the non-ideal effect of the MIS structure.

$\rho'(x)$ can be written as

$$\rho'(x)=\rho(x)+\delta(d)Q_{ss},$$

where $\delta(d)$ is a delta function.

Considering these non-ideal effects, the threshold voltage can be modified as

$$V_T=V_{FB}+2\Phi_F - \frac{Q_B}{C_0}, \qquad (2)$$

where

$$V_{FB}= - \frac{1}{C_0} \int_0^d \frac{x}{d} \rho(x)dx + \frac{W_{ms}}{e} - \frac{Q_{ss}}{C_0},$$

d is the thickness of the insulator, and x the position along the axis shown in Figure 2.2.

V_{FB} is the non-ideal-effects modification term. If V_{FB} were applied to a non-ideal MIS structure, then its band structure could be considered equivalent to a flat band structure without any applied external voltage. The subscript FB implies the Flat Band.

§2.2. The Operational Principle of the IGFET and the ISFET

1. The IGFET

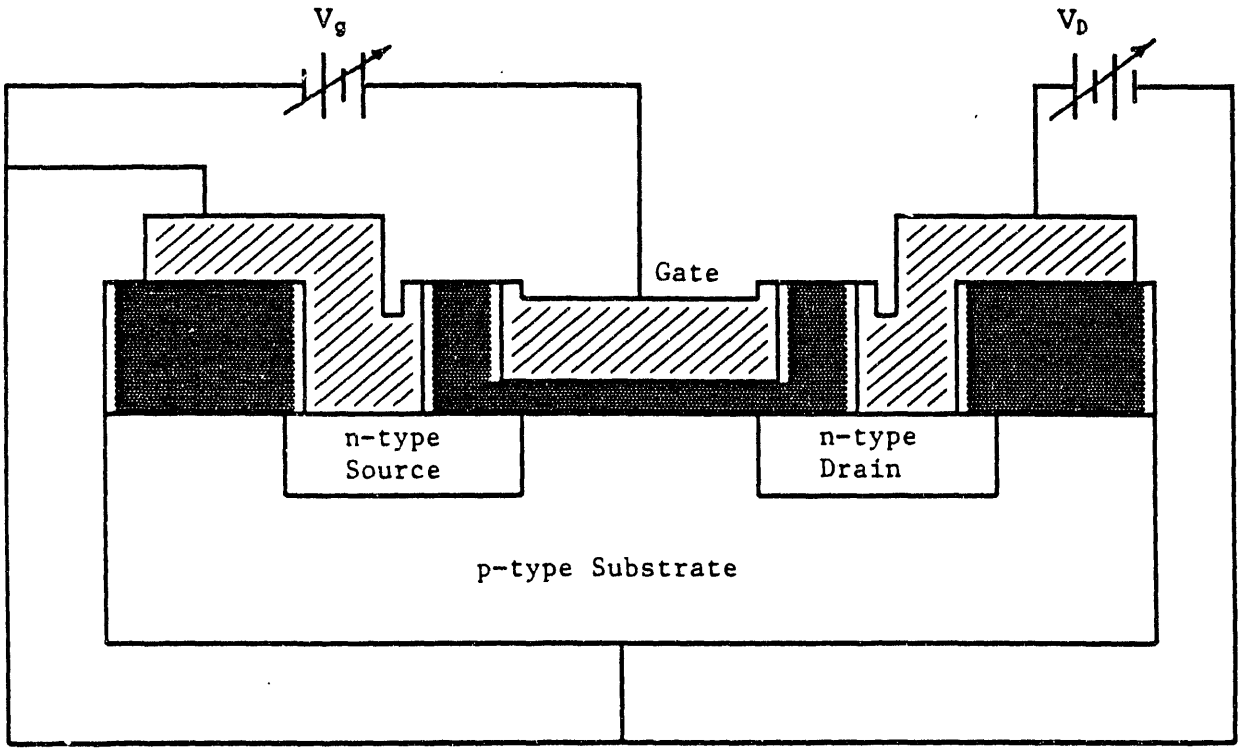

Figure 2.5 Schematic Diagram of an IGFET. ▒, metal; ▓, insulator

The structure of an IGFET is shown by Figure 2.5. It is essentially an MIS structure. From the analysis of the MIS structure in §2.1, we know that the operational principle of the IGFET is the modulation of electrical

conductivity of the surface channel by the applied voltage V_g.

As shown in Figure 2.5, both the drain and the source regions of the IGFET are n-type semiconductors. They form p-n junctions on the interfaces with the p-type semiconductor substrate. Under depletion or accumulation biasing conditions, there is no electric current between drain and substrate or between source and substrate because of the reverse biased p-n junction, so drain-source current is zero. Only when V_g is sufficiently large to make the semiconductor invert is the conducting channel formed (Figure 2.6), and the drain voltage V_D applied between drain and source causes drain current I_D to flow in the conducting channel.

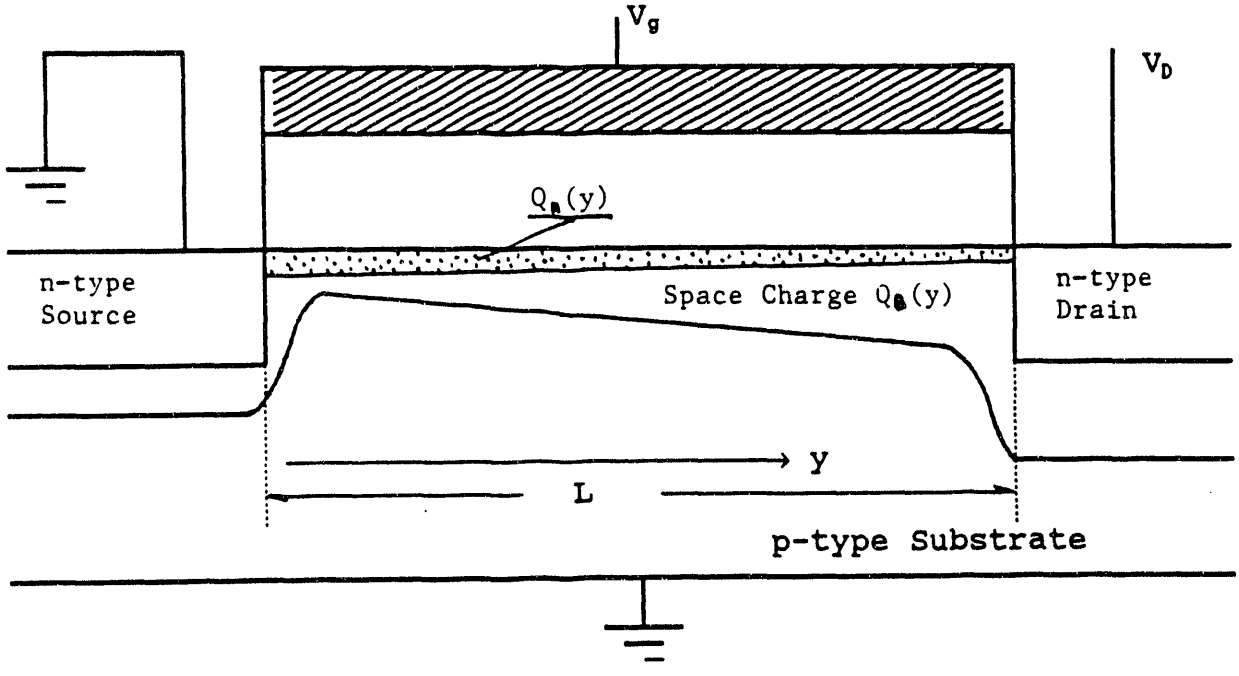

Figure 2.6 IGFET Conducting Channel. ▨ indicates the metal

▨ indicates the conducting channel

According to Ohm's law, the potential difference dV across an infinitesimal distance dy between the source and drain is given by

$$dV = I_D dR = \frac{I_D dy}{b\mu_n Q_n(y)}, \tag{3}$$

where dR is the resistance across dy, b is the width of the channel, μ_n is the electron mobility in the channel, and $Q_n(y)$ is the charge density of mobile electrons in the conducting channel.

In addition to the mobile electrons. there are also ionized dopant atoms of charge density $Q_B(y)$ in the surface charge region. We thus have a total surface charge density $Q_s(y)$ given by

$$Q_s(y) = Q_n(y)+Q_B(y) .$$

As a result,

$$V_g - V_{FB} = - \frac{Q_s}{C_0} + \Phi_s ,$$

where Φ_s is the surface potential of the semiconductor. Hence,

$$Q_n(y) = - [V_g - V_{FB} - \Phi_s(y)]C_0 - Q_B(y) . \tag{4}$$

For strong inversion,

$$\Phi_s(y) = V(y) + 2\Phi_F ,$$

where V(y) is the voltage drop along the channel.

Under the depletion approximation, which assumes that there are no mobile charges in the space-charge regions, $Q_B(y)$ can be written as

$$Q_B(y) = - \{2K_s\varepsilon_0 q N_A [V(y)+2\Phi_F]\}^{1/2} , \tag{5}$$

where K_s is the dielectric constant of the semiconductor and N_A is the number of the dopant atoms per unit volume. Then $Q_n(y)$ becomes

$$Q_n(y)= - [V_g - V_{FB} - V(y) - 2\Phi_F]C_0+\{2K_s\varepsilon_0 qN_A[V(y)+2\Phi_F]\}^{1/2} . \qquad (6)$$

Note that $V_T=V_{FB}+2\Phi_F - \frac{Q_B}{C_0}$; thus $V_{FB}+2\Phi_F=V_T - \frac{Q_B}{C_0}$

and $Q_n(y)= - [V_g - V_T - V(y)]C_0 .$

The mobile electron density, $Q_n(y)$, in the inversion layer surface thus becomes a linear function of $(V_g - V_T)$ when $V_g > V_T$, the latter given by the equation (6).

From Ohm's law,

$$dV= \frac{I_D dy}{b\mu_n Q_n(y)}$$

Combining the two previous equations and integrating (note that in most cases V_T can be treated as a constant although it is a function of y), we have

$$I_D=\mu_n C_0 \frac{b}{L} [(V_g - V_T)V_D - \frac{V_D^2}{2}] \quad [V_D<V_{DSAT}] , \qquad (7)$$

for drain voltages below saturation, and

$$I_D=\mu_n C_0 \frac{b(V_g - V_T)^2}{2L} \quad [V_D>V_{DSAT}] , \qquad (8)$$

above saturation. In Equation (7)-(8), L is the length of the channel.

Further, $V_T = V_{FB} + 2\Phi_F - \frac{Q_B}{C_0}$ and $V_{FB} = \Phi_{ms} - \frac{Q_{ss}}{C_0}$; thus, $V_{DSAT} = V_g - V_T .$

where V_{DSAT} is the threshold voltage of the saturation of the IGFET. Saturation means that when V_D is sufficiently large, $V_D \geq V_{DSAT}$, I_D will not increase as V_D does. Figure 2.7 illustrates the saturation condition of the IGFET and Figure 2.8 shows the I_D-V_D characteristics curve of the IGFET.

2. The ISFET

Compare Figure 2.1 (the structure of the ISFET) and Figure 2.5 (the structure of the IGFET). The differences between them are that the gate in the IGFET is replaced by a 'remote' reference electrode in ISFET, and there is an ion-sensitive membrane on the top of the insulator and an encapsulant which protects the ISFET. A potential difference between the membrane and the semiconductor must be considered.

The ISFET can be considered to have six phases in a single mutiphase system. From the Gibbs' equation,

$$\Sigma dn_i \tilde{a}_i = 0 ,$$

where dn_i is the number of species i which are transported across each of the interfaces, $\tilde{a}_i$ is the electrochemical potential of species i. At equilibrium,

$$\tilde{a}_1 \equiv \tilde{a}_2 \equiv \tilde{a}_3 \equiv \tilde{a}_6 \equiv \tilde{a}_5 . \qquad (9)$$

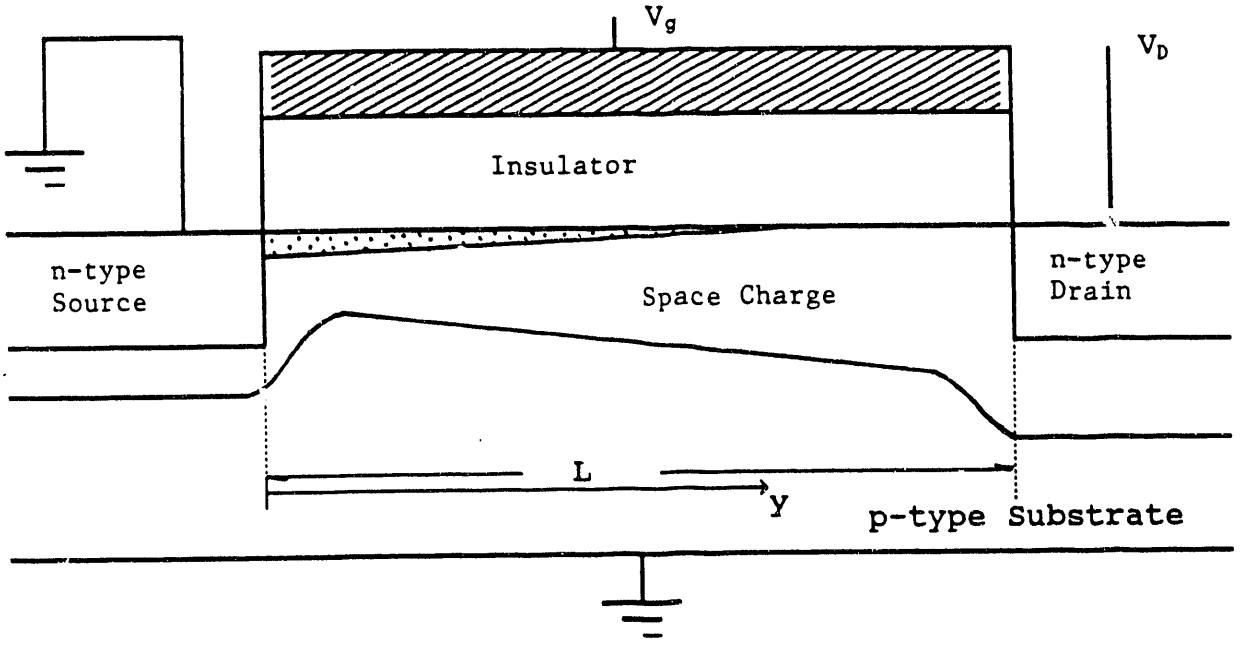

Figure 2.7 IGFET Saturation

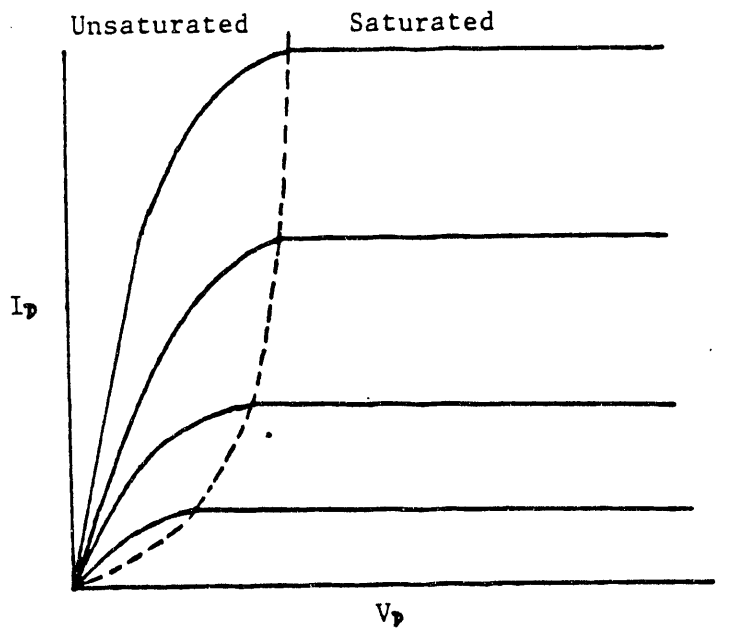

Figure 2.8 I_D/V_D Curve of the ISFET

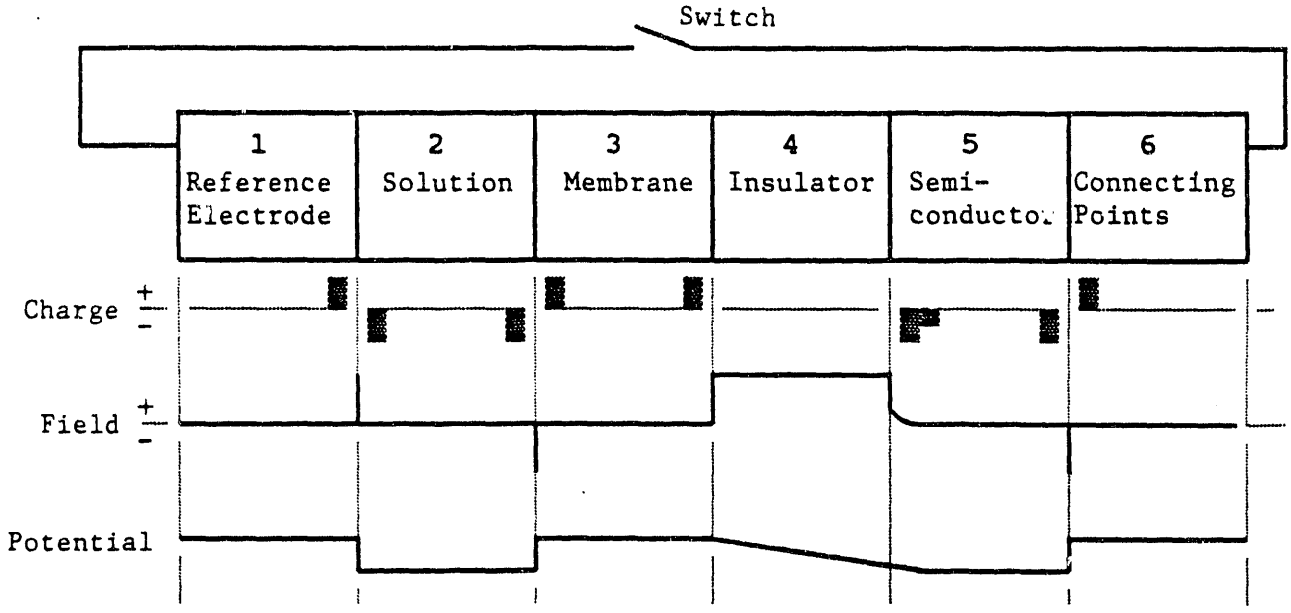

Figure 2.9 Charge, Field and Potential Profiles of the ISFET Gate

In Figure 2.9, box 1 represents the reference electrode, a metal which is described by the equilibrium equation:

$$M = M^{+}+e^{-},$$

Box 2 stands for the solution which contains the ions to be detected. Box 3 is the membrane which is on the top of the insulator. Box 4 is the insulator which is assumed to be an ideal insulator. Box 5 indicates the semiconductor such as silicon. Box 6 is the metal that forms the connecting points of the drain and source poles.

Note that in Equation (9), $\tilde{a}_4$ is missing, since there is no electrochemical potential in the ideal insulator. Equation (9) can only exist (the equilibrium state) when the switch (in Figure 2.9) is closed. If the switch is open, which means the absence of the electrode reference, there is no way to let $\tilde{a}_3$ equal to $\tilde{a}_5$, therefore, the system cannot reach equilibrium,

this means that the FET cannot operate. Thus, a reference electrode is the basic requirement for the operation of an ISFET.

The inner potential of the semiconductor is

$$U_5 = \frac{1}{F}(a_5^e - \tilde{a}_5^e) \ .$$

The superscript e indicates the electron, a_5^e is the electron-lattice interaction energy in the semiconductor, $\tilde{a}_5^e$ is the electrochemical potential of an electron in phase 5, the Fermi level, and F is the Faraday constant.

The inner potential of the membrane U_3 is

$$U_3 = \frac{1}{Z^i F}(\tilde{a}_3^i - a_3^i),$$

where the Z^i is the number of elementary charges, it is positive for cations and negative for anions. $\tilde{a}_3^i$ and a_3^i are the electrochemical and the chemical potentials respectively of species i in phase 3.

Therefore, the potential difference of the space-charge regions across the insulator is

$$\Delta\Phi_{53} = \Delta U_{53} = U_5 - U_3 = \frac{1}{F}[(a_5^e - \tilde{a}_5^e) - \frac{1}{Z^i}(\tilde{a}_3^i - a_3^i)] \ . \qquad (10)$$

Since ion i can transfer from the solution to the membrane, at equilibrium we have

$$\tilde{a}_3^i = \tilde{a}_2^i = a_2^i + Z^i F U_2 \ , \text{ and } \tilde{a}_5^e = \tilde{a}_1^e = a_1^e - F U_1 \ , \qquad (11)$$

Since $M_1 = M_1^+ + e^-$, $a_1^M = a_1^{M^+} + a_1^e$, hence $a_1^e = a_1^M - a_1^{M^+}$.

Substituting a_1^e in to equation (11), we have

$$\tilde{a}_5^e = a_1^M - a_1^{M^+} - FU_1 \ . \qquad (12)$$

Combining equations (10), (11) and (12) yields

$$\Delta U_{53} = \frac{1}{F}(a_5^e - a_1^M + a_1^{M^+}) - \frac{1}{Z^i F}(a_2^i - a_3^i) + (U_2 - U_1) \ . \qquad (13)$$

Note that

$$\frac{1}{F}(a_5^e - a_1^M + a_1^{M^+}) = \frac{1}{F}(a_5^e - a_1^e) = U_5 - U_1 = -\Delta\Phi_c,$$

so the first term of equation (13) is the negative value of the contact potential, $-\Delta\Phi_c$, between the semiconductor and the metal. By using the Nernst equation, the second term of equation (13) can be written as

$$\frac{1}{Z^i F}(a_2^i - a_3^i) = E_0^i + \frac{RT}{Z^i F}\ln\alpha_2^i \ .$$

Where α_2^i is the ion activity in the solution. The ion activity of the membrane, α_3^i, is assumed to be constant and is included in E_0^i.

The last term of equation (13), $(U_1 - U_2)$, is the reference electrode potential E_{ref}. Thus, rewriting equation (13), we have

$$\Delta U_{53} = -\Delta\Phi_c - E_0^i - \frac{RT}{Z^i F}\ln\alpha_2^i + E_{ref} \ . \qquad (14)$$

Since ΔU_{53} is the potential difference between the membrane and the semiconductor, $\Delta U_{35} = -\Delta U_{53}$ should be added to V_g, when we consider the relationship between the drain current and the drain voltage. Then equation (7) becomes

$$I_D = \frac{\mu_n C_0 b V_D}{L}\left(V_g + \Delta\Phi_c + E_0^i + \frac{RT}{Z^i F}\ln\alpha_2^i - E_{ref} + \frac{Q_{ss}}{C_0} - 2\Phi_F + \frac{Q_B}{C_0} - \frac{V_D}{2}\right)$$

and the threshold voltage of the ISFET is re-defined as

$$V_T = - \Delta\Phi_c - E_0{}^i - \frac{Q_{ss}}{C_0} + 2\Phi_F - \frac{Q_B}{C_0} .$$

The final equation for the drain current of the ISFET sensitive to the activity of ions i is

$$I_D = \frac{\mu_n C_0 b V_D}{L} \left(V_g - V_T \pm \frac{RT}{Z^i F} \ln\alpha_2^i - E_{ref} - \frac{V_D}{2}\right) , [V_D < V_{DSAT}], \quad (15)$$

and $$I_D = \frac{\mu_n C_0 b}{2L} \left(V_g - V_T \pm \frac{RT}{Z^i F} \ln\alpha_2^i - E_{ref}\right) , [V_D > V_{DSAT}]. \quad (16)$$

§2.3. ISFET Selectivity

Selectivity refers to the fact that the sensor has the ability to respond primarily to only one species of ions while there are other species of ions present. The sensor output is a combination of the contributions of the interactions of several different kinds of ions. The primary contribution is from one dominate species S, and the effects of the other species of ions (interfering species) can often to be minimized. This may be represented by the expression

$$V_{OUT} = V(S, \Sigma_k S_k) .$$

In the case of an ISFET, ion selectivity results from the ion selective membrane. The membrane has a permeability to certain kinds of ions. When the electrochemical potentials of the ions are the same on each side of the membrane, the system reaches equilibrium. The partitioning of the ions between the solution and the membrane results in a potential difference, E_{OUT}, between

these two phases. So, E_{OUT} is related to the activities of the partitioning ions rather than to their concentrations. Generally, E_{OUT} can be expressed by the Eisenmann-Nikolskij equation [24]

$$E_{OUT}= \frac{RT}{Z_j F} \ln(\alpha_j+\Sigma_k K_{j,k}\alpha_j^{Z_j/Z_k}) , \qquad (17)$$

where R is the gas constant, T is the absolute temperature, $K_{j,k}$ is the selectivity coefficient, a unitless constant that may be determined by the comparison of the electrode response to a solution containing only the primary ion at activity α_j with that containing α_k of the interference as well as α_j of the primary ion. j and k indicate the dominate and interfering species of ions, respectively. Z_j is the charge number of the species j ions, and α_j is the ionic activity of j ions. E_{OUT} is superimposed over the reference electrode potential. It is this term that brings ion selectivity.

The I_D–V_D relationship thus can be expressed as

$$I_D = \frac{\mu_n C_0 b V_D}{L}\left[V_g - V_T - E_{ref} - \frac{V_D}{2} + \frac{RT}{Z_j F}\ln(\alpha_j+\Sigma_k K_{j,k}\alpha_j^{Z_j/Z_k})\right]. \qquad (18)$$

When temperature is fixed, E_0^i is a constant, thus V_T is a constant. Assuming that α_{Cl^-} in the solution does not change, then E_{ref} becomes a constant [25]. Under constant I_D and V_D operations,

$$V_{out}= V_g = \beta - \frac{RT}{Z_j F}\ln(\alpha_j+\Sigma_k K_{j,k}\alpha_j^{Z_j/Z_k}),$$

$$\text{where } \beta = \frac{I_D L}{\mu_n C_0 b V_D} + V_T + E_{ref} + \frac{V_D}{2} \text{ is a constant.}$$

It is this V_{out} that is measured in the experiments that follow.

CHAPTER 3. EXPERIMENTAL

This chapter describes three main systems: (1) The ISFET pH probe which consisted of a Ag/AgCl reference electrode and an ISFET. This part will be described in §3.1. (2) The temperature and pressure control systems whose function was to provide the high temperature and high pressure conditions in a test cell. Since the pH value is a function of temperature and pressure, it is a very important part of the experiment, and will be described in §3.2. (3) The data collecting system which consisted of an amplifier and a precision multimeter (Fluke); they will be discussed in §3.3.

Three groups of experiments were performed. They were measurements of the ISFET's output as a function of (1) time at fixed pH; (2) temperature at atmospheric pressure; (3) pressure at several temperatures.

§3.1. The pH Probe

1. Reference Electrode

The Ag/AgCl reference electrodes were prepared from a silver wire (one millimeter in diameter) which was electrochemically coated with silver chloride. The fabrication procedure consisted of two steps:

(1). An apparatus was set up as shown below:

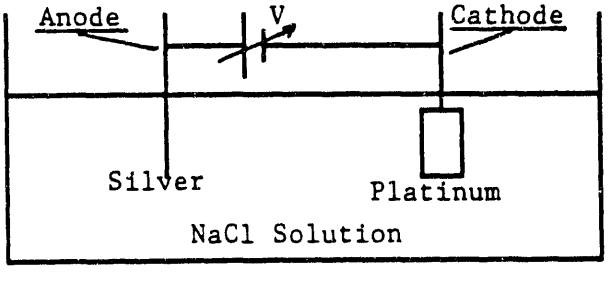

Figure 3.1 Preparation of the Ag/AgCl Reference Electrode

(2). The voltage V was increased very slowly until tiny H_2 bubbles appeared on the platinum cathode. The reaction was allowed to proceed at this voltage until the silver wire was uniformly coated with AgCl. This completed the electroplating.

The anode reaction is

$$2Ag_{(s)} + 2H^{+}_{(g)} + 2Cl^{-}_{(g)} \longrightarrow 2AgCl_{(s)} + H_{2(g)}.$$

2. The ISFET Probe

As shown in Figure 3.1, the ISFET and the Ag/AgCl reference electrode were mounted together to form a probe. Epoxy resin was used to fix the ISFET and Ag/AgCl reference electrode in the shell of the probe. The epoxy was applied in such a manner that it covered every part of the lead wires of drain and source poles but not any part of the membrane of the ISFET. If the lead wires were exposed to the solution, thermal expansion would loosen the sealant between the wire and the physical part of the ISFET, allowing solution to enter the ISFET and destroy it. If any epoxy was put on the membrane of the ISFET, it would prevent contact between the membrane and the solution. The epoxy forms the pressure seal for the probe. A three lead connector was used to connect the Ag/AgCl reference electrode, the drain and source leads of the ISFET. To reduce the noise, shielded wires were used to connect the probe to the amplifier.

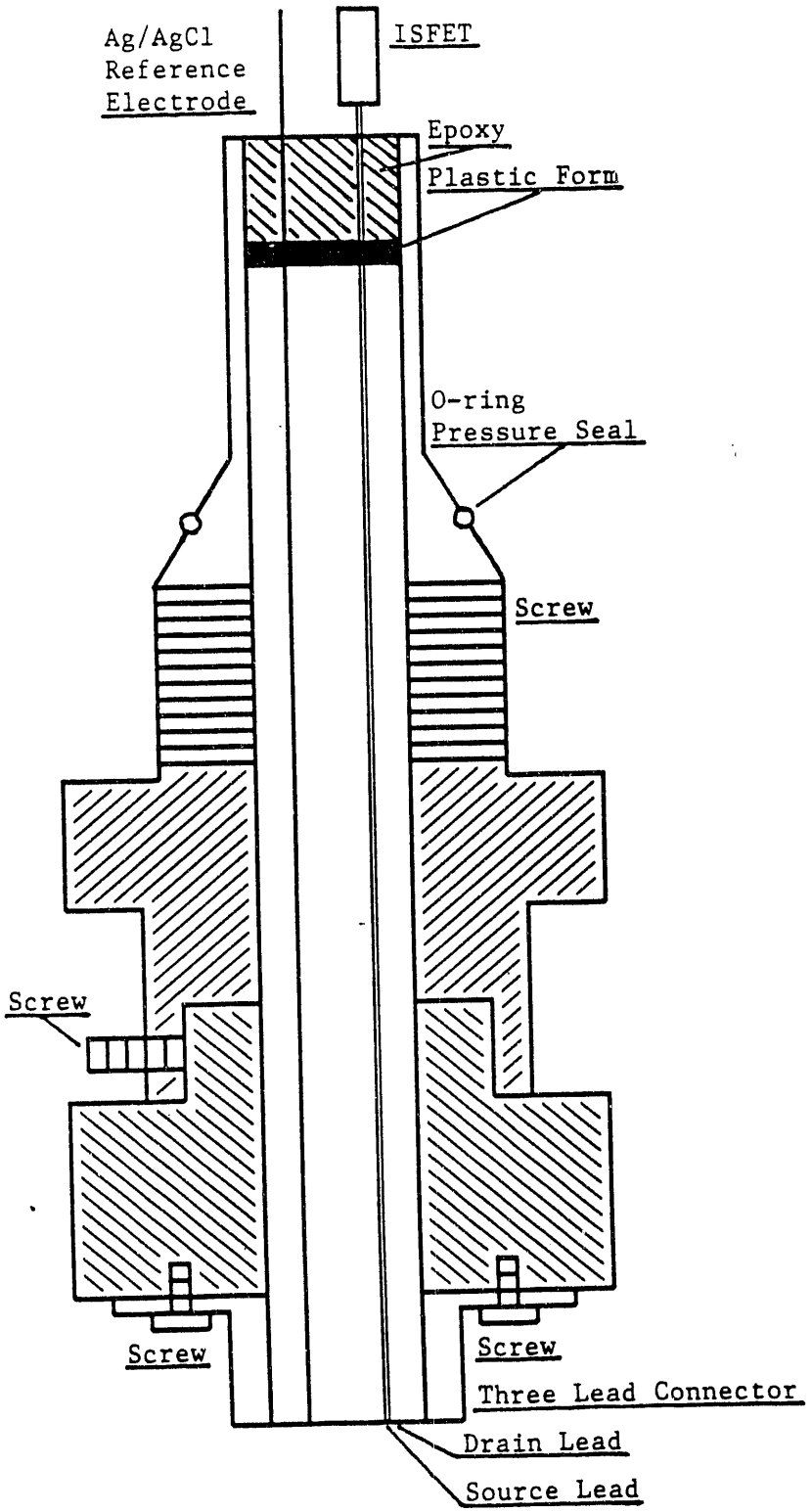

Figure 3.2 The pH Probe

§3.2. The Pressure and Temperature Control System

These system were used to control the temperature and the pressure of test solutions. The system is shown in a block diagram below:

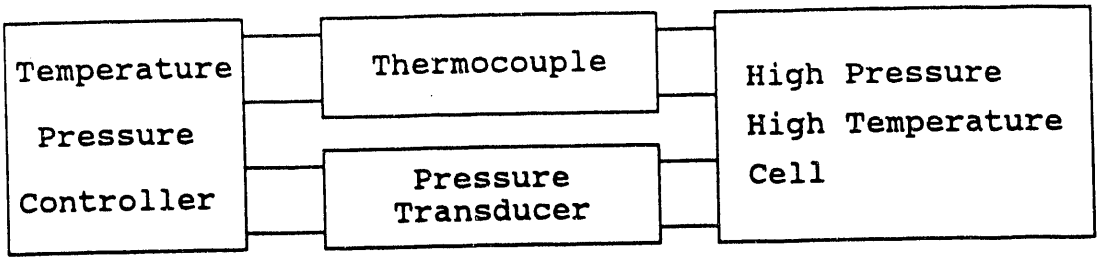

Figure 3.3 The Pressure and Temperature Control System

1. Pressure Control System

(1). The high pressure and high temperature cell:

A high pressure/high temperature cell was designed by Dr. D. F. Keeley and made as shown in Figure 3.3. The diameter of the piston is one and half inches (about 0.0381 meter). There are four ports in the wall of the cell which were used to put an ISFET probe, a pressure transducer and the other kinds of sensors in the cell as needed. An Omega iron/constantan J type thermocouple was put in a small hole in the wall of the cell. A channel and a screw on the piston were used to bleed the solution so that any air in the solution can be forced out of the cell. Figure 3.4 shows the high pressure cell with pressure transducer and thermocouple assembly.

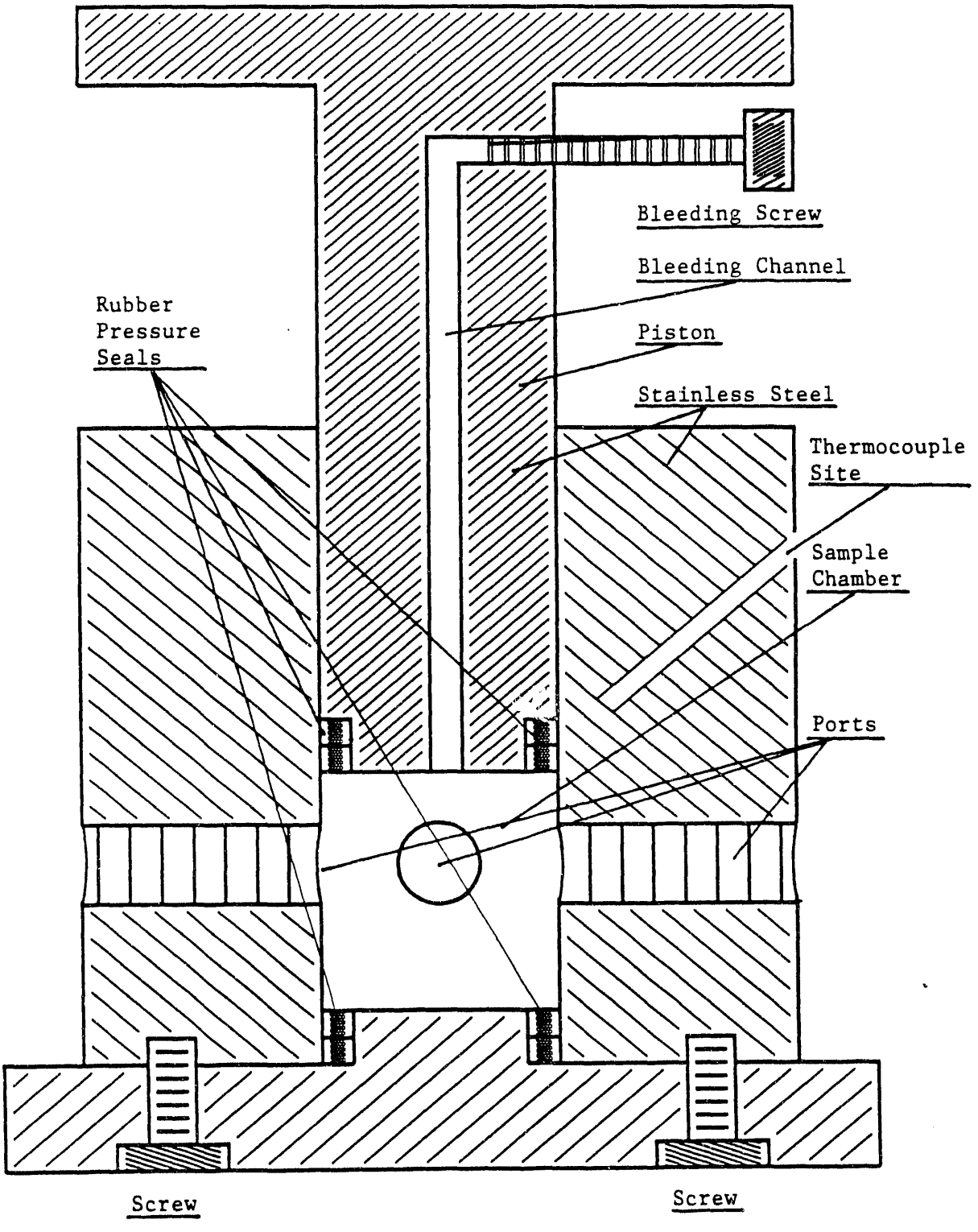

Figure 3.4 The High Pressure Cell

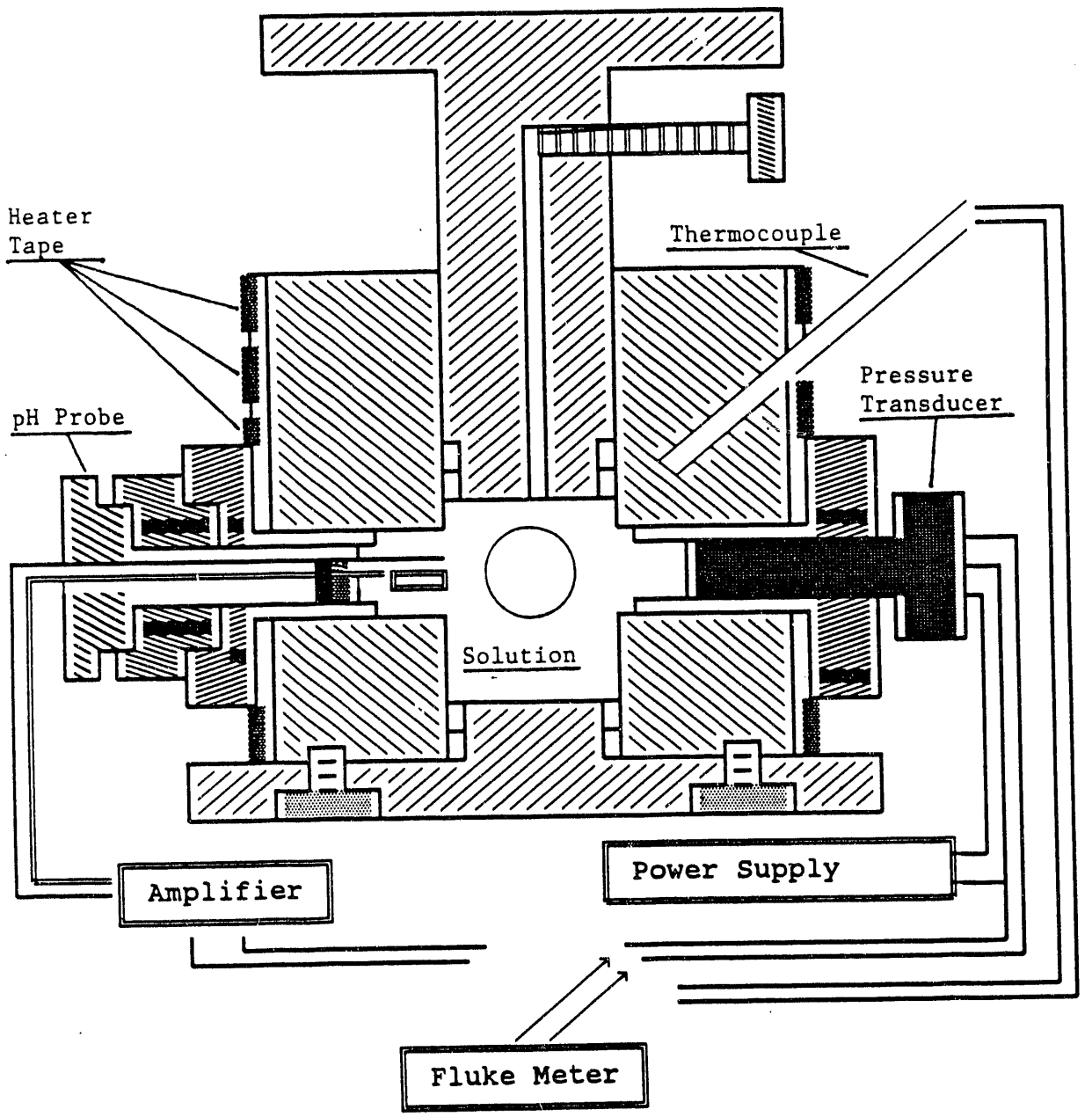

Figure 3.5 High Pressure Cell with ISFET, Pressure Transducer and Thermocouple

(2) Pressure generator

A Carver Laboratory Press (Model: M) with an adjusting range from zero to 200 kN was applied to the piston to produce the high pressure, thus the high pressure cell can generate a pressure of more than 176 MPa. A hydraulic controller preset and automatically maintained the pressure. An Omega PX303-10K65V pressure transducer was put in the high pressure cell in order to measure the pressure. The pressure transducer was calibrated by M-Tec/Rise, Inc. using dead weight test, and the curve is shown in Figure 3.8.

2. The Temperature Control System

A heating tape and an Omega CN7100 temperature controller were used to raise and control the temperature of the cell. The tape was wound on the high pressure cell and a thermocouple was put in the small hole on the high pressure cell as shown in Figure 3.5. The temperature could be adjusted over the range of the experiment (from room temperature to 250°C). The thermocouple was calibrated by a CMS precision thermometer and the calibration data and curve are shown in Table 12 and Figure 3.9.

§3.3. The Measurement System

1. Amplifier

The function of the measuring circuit is to detect and amplify the electrochemical potential changes between the semiconductor and the solution. The ISFET should work under maximum ion sensitivity, i.e., a every small change in ion concentration of the solution should be reflected in a drain current change of the ISFET. This requires that the ISFET is unsaturated and under strong inversion since when the ISFET is saturated, I_D will be a

constant no matter how V_D changes. On the hand, when the FET is strongly inverted, the semiconductor yields the maximum number of mobile electrons, and the channel has the maximum conductivity. Under this situation a change in the activity of the ions in the solution will be reflected as a change in the number of mobile charge carriers in the conducting channel (field effect).

There are two types of measuring methods: (1) constant gate voltage V_g operation: the gate voltage V_g is held constant and the change of drain current is measured directly; and (2) constant drain current I_D operation: varying the gate voltage such to hold drain current constant.

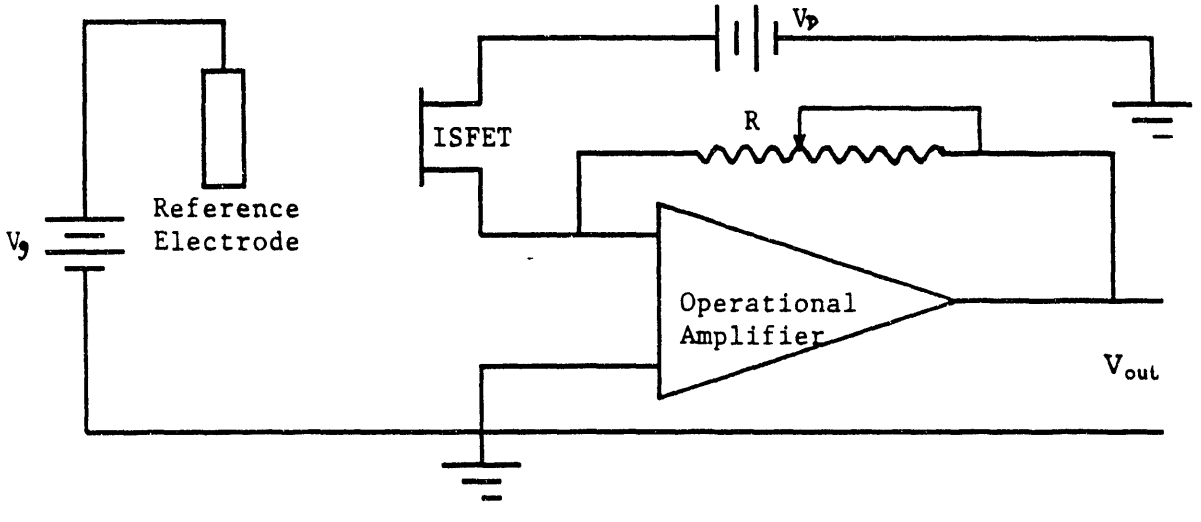

Figure 3.6 Schematic of Circuit Diagram for Constant V_g Operation Amplifier

(1). Constant Gate Voltage Operation

The circuit diagram is shown in Figure 3.6. Although the technique is simple, this design has a disadvantage in that the ISFET is not an ideal device, non-ideal effects will cause the relation between the drain current and system voltages to be different from that predicted by the Equation 15 in

Chapter 2. This requires a calibration over its total operating range. For any different configuration, the different calibration is needed.

(2). Constant Drain Current Operation

In this mode of operation, the change of electrochemical potential between the solution and semiconductor is read out directly. Using an operational amplifier with a feedback loop, a change of voltage resulting from the change of ionic activity will be reflected as a change of gate voltage, thus the drain current can be held constant. In this situation, any non-ideal effect will be held constant, so the calibration is not necessary for every design. The circuit diagram of constant drain current operation is shown in Figure 3.7.

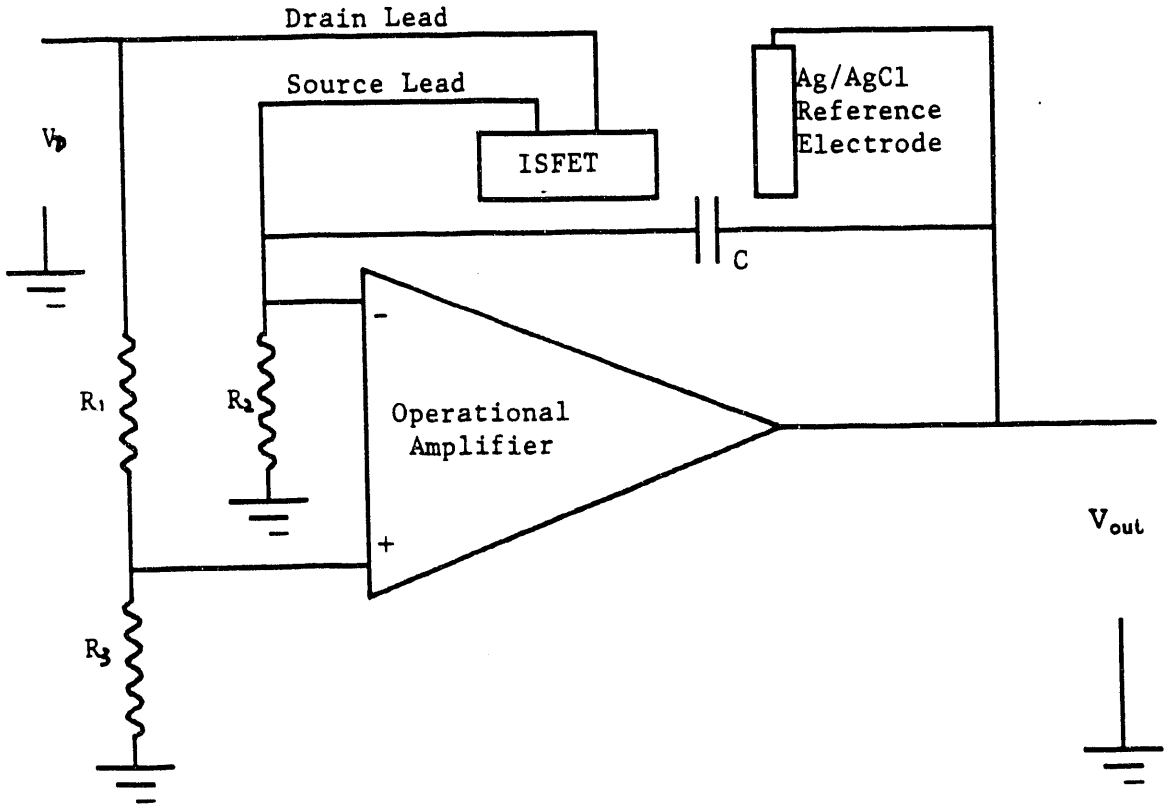

Figure 3.7 Principal Circuit Diagram of the Amplifier

In our experiment, the ISFET output signal is processed by an amplifier which was bought from Chemfet Corp.. The amplifier, shown in Figure 3.7, operates with a constant drain current.

2. Data Collecting System

At the beginning of the research, we used a computer data collecting system. The system consisted a DAS-8PGA eight-channel data interface board and LABTECH Acquire software which was run by an AT personal computer. The advantages of this system are that sampling rates can be precisely set and that all data acquisition and data analysis was part of or read into the software. We found that there were some disadvantages of the system. There was some unknown noise which was difficult to eliminate, and with the Acquire software there was a nine hours and six minutes running limit (no matter how the sampling frequency was set). We wished to run a much longer term of measurement. With these disadvantages, we abandoned this system and used a precision multimeter to measure the output voltages.

§3.4 Experiment

A series of sodium chloride solutions buffered to pH values ranging from 4 to 10 were prepared using $NaH_2PO_4 \cdot H_2O$ as the acid and $Na_2HPO_4 \cdot 7H_2O$ as the base. The concentration of the reference salt NaCl was 0.1 M. The buffer strength was 0.05 M. A CORNING pH meter (model 10) was used as a calibration device.

The first five ISFETs received from Chemfet Corp. were labeled 1-5 and were calibrated using the buffer solutions. The results are shown below. A later group we received had a manufacturer's reference number which was used

to identify them.

FET No:	Slope (V_{out}(V)/pH unit)
1	0.0464
2	0.0434
3	0.0469
4	0.0470
5	0.0467

The results for the calibration of ISFET 3039 is in Table 13 and Figure 3.28-33. Data analysis was performed and the results are shown on the figures. The data indicates a linear relationship between the ISFET output and the pH value.

1. Stability Tests of the ISFET:

The first long term test (labeled S-1) was made from Jan. 9, to Jan. 19, 1990, using ISFET 3 in a pH 4.05 buffered solution. The sampling frequency was eight hours. The temperature of the solution was maintained at 25°C in a thermostated constant temperature bath. A precision multimeter was used to measure the ISFET output V_{out}. The result is presented in Table 1 and Figure 3.10.

The second, longer stability test (labeled S-2) using ISFET 3039 was made from Dec. 18, 1990 to Mar. 13, 1991, in a pH 5.29 buffered solution, sampling about every twelve hours. The buffered solution was put in the high pressure cell but was neither pressured nor thermostated. The results are shown in Table 2 and Figure 3.11.

2. ISFET Output as a Function of Temperature:

These experiments were performed at atmospheric pressure. The temperature of the solution was controlled by a constant temperature bath. Due to the ISFETs' failures during these experiments, we did not obtain much data under these conditions. The malfunction of the ISFET may have been due to improper fabrication of the ISFET, the drain and source leads of the ISFET may have opened due to thermal expansion or the solution may have entered the physical part of the ISFET and shorted it.

Experiment T-1: A pH probe (labeled R) which was provided by Chemfet Corp. was used in this experiment with pH 4.05 buffered solution. The result was tabulated by Table 3 and Figure 3.12.

Experiment T-2: ISFET 3021 was used with pH 5.26 buffered solution. The result was shown in Table 4 and Figure 3.13.

3. ISFET Output as a Function of Pressure:

There are two sub-groups of experiments:

(1). The temperature of the buffered solutions were not thermostated. The experiments were performed at room temperature, around 25°C.

A precision multimeter was used to measure the outputs of the ISFET probe and pressure transducer. ISFETs 3041 and 3049 were used in these experiments. Different pH values of buffered solutions, pH=5.26, 6.27 and 7.29, were tested under room temperature using ISFET 3041 and the experiments were repeated.

In an another experiment, the output of ISFET (3041) in a pH 6.84 buffered solution was measured as a function of pressure, and the results are shown in Table 5 and Figure 3.14. Table 8 and Figure 3.21 show the experiments with ISFET 3049 in a pH 6.27 buffered solution.

The experiments are listed in following table:

Label	Experiment	Results shown in
P-1	ISFET 3041, pH 6.84, 6/7/90	Table 5, Figure 3.14
P-2	ISFET 3041, pH 5.26, 6/13/90	Table 6, Figure 3.15
P-3	ISFET 3041, pH 6.27, 6/13/90	Table 6, Figure 3.16
P-4	ISFET 3041, pH 7.29, 6/13/90	Table 6, Figure 3.17
P-5	ISFET 3041, pH 5.26, 6/15/90	Table 7, Figure 3.18
P-6	ISFET 3041, pH 6.27, 6/15/90	Table 7, Figure 3.19
P-7	ISFET 3041, pH 7.29, 6/15/90	Table 7, Figure 3.20
P-8	ISFET 3049, pH 6.27, 8/15/90	Table 8, Figure 3.21

(2). The temperature of the test solutions in the high pressure cell were set and maintained by the temperature controller. At six different temperatures, between 26°C and 70°C, the ISFET output was measured as a function of pressure, The pH of the solutions was either 5.26 or 6.27. The results of the experiments are shown below:

Label	Experiment	Results shown in
PT-1	ISFET 3041, pH 5.26, 40°C, 7/6/90	Table 9, Figure 3.22
PT-2	ISFET 3041, pH 5.26, 50°C, 7/6/90	Table 9, Figure 3.23
PT-3	ISFET 3041, pH 5.26, 60°C, 7/6/90	Table 9, Figure 3.24
PT-4	ISFET 3041, pH 5.26, 70°C, 7/6/90	Table 9, Figure 3.25
PT-5	ISFET 3049, pH 6.27, 26°C, 8/16/90	Table 10, Figure 3.26
PT-6	ISFET 3049, pH 6.27, 37°C, 8/16/90	Table 10, Figure 3.27

§3.5 Data Analysis

Since the measurement devices were not ideal devices, there were

measurement errors in the data. Therefore, all of the data was considered to be random variables. We used linear regression to analyze these data since they seem to be linear from the graphics. The statistical results confirm this.

In order to show these linear relationships analytically, we employ two statistical tests: coefficient of correlation R and t-test.

1. Linear Regression

This method of curve fitting is one of a number of processes in mathematics which use finite differences. We can find a best fit straight line for a set of sample points by using this method. Suppose that we have n points ($X_1, X_2, \ldots X_n$ and $Y_1, Y_2, \ldots Y_n$) and want to fit them into a straight line,

$$Y = a + bX \ ,$$

to them. δ_i is defined as

$$\delta_i = Y_i - (a + bX_i) \ .$$

So
$$D = \sum_{i=1}^{n} \delta_i^2 = \sum_{i=1}^{n} (Y_i - a - bX_i)^2 \ .$$

We can then choose a and b to yield a minimum D, such that $Y = a - bX$ is the best fit straight line of these n points $\{X_i, Y_i\}_n$. The minimization is performed by setting

$$\frac{\partial D}{\partial a} = \sum_{i=1}^{n} -2(Y_i - a - bX_i) = 0 \ ,$$

and
$$\frac{\partial D}{\partial b} = \sum_{i=1}^{n} -2X_i(Y_i - a - bX_i) = 0 \ .$$

Collecting terms

$$na+b\sum_{i=1}^{n} X_i=\sum Y_i$$

and

$$a\sum_{i=1}^{n} X_i+b\sum_{i=1}^{n} X_i^2=\sum_{=1}^{n} X_iY_i \ .$$

Then, we have

$$b=\frac{SSXY}{SSX^2} \ ,$$

and

$$a=\bar{Y}-b\bar{X} \ ,$$

where

$$\bar{X}=\sum_{i=1}^{n} X_i/n, \text{ and } \bar{Y}=\sum_{i=1}^{n} Y_i/n \ ,$$

$$SSXY=\sum_{i=1}^{n} X_iY_i-\frac{\Sigma X_i \Sigma Y_i}{n}=\sum_{i=1}^{n} X_iY_i-\bar{X}\sum_{i=1}^{n} Y_i \ ,$$

and

$$SSX^2=\sum_{i=1}^{n} X_i^2-\frac{(\Sigma X_i)^2}{n}=\sum_{i=1}^{n} X_i^2-\bar{X}\sum_{i=1}^{n} X_i \ .$$

The *Standard Deviation of the Estimated Y* is defined as

$$s(Y)=\left[\frac{\sum_{i=1}^{n}(Y_i-a-bX_i)}{n-1}\right]^{1/2} \ ,$$

and the *Variance of Slope b* is

$$s^2(b)=s^2(Y)/\ SSX^2 \ ,$$

and the *Variance of Mean* of *Y* is

$$s^2(\bar{Y})=s^2(Y)/n \ .$$

The *Coefficient of Correlation* is defined as

$$R = \frac{SSXY}{\sqrt{SSX^2 SSY^2}} .$$

So, if $R^2 = 0.9$, we can say that 90% of the variation in the data is explained by the line $Y=a+bX$. We also can check with a correlation coefficient table, Table 14 [26], to see if there is a correlation between X and Y.

The confidence limits of the, say, mean of the Y's is:

$$\bar{Y} = \bar{Y} \pm t_A s(\bar{Y}) ,$$

where t_A can be obtained from t-table [27] and A is the percent confidence range.

2. Analysis

A confidence range 95%, A=0.05, was chosen in data analysis below. Details of the calculations are shown under stability tests and only in tabular form there after.

(1). Calibration of ISFET 3039

In Figures 3.28-3.33, we can see that $R^2 > 0.98$ for all of six sets of data. So, we say that over 98% of the data were presented by the best fit lines. Since $R > 0.99$, from Table 14, we know that for two degrees of freedom we say with 99% confidence that the output of the ISFET has a linear relationship with the pH value.

(2). Stability Tests of ISFET

Using the data in Figure 3.9 and Table 1 and performing a regression analysis, we have $R^2 = 0.83$, $R = 0.91$, $n = 29$. According to Table 14, we are over 99.9% confident that the relationship between the ISFET output and time is a linear function; 83% of the data points are presented by the best fit line:

$$V_{out}(v) = 9.88964\times10^{-5}t+3.1489$$

Choose A=0.05, that is, 95% of confidence, the degrees of freedom, n-1=28. Refer to a t-value table of a statistics book [26], t_A=2.05, thus the confidence limit of V_{out} is:

$$\delta V_{out}=t_A s(V_{out})=2.05\times0.003705=0.00769 \text{ V} ,$$

$$\delta b=t_A s(b)=2.05\times0.000009=1.845000\times10^{-5}\text{V/hours} .$$

So, we can say with 95% confidence that:

$$V_{out}=9.88964\times10^{-5}t+3.1489\pm0.00769 \text{ V} ,$$

and $$b=(9.88964\pm1.84500)\times10^{-5}\text{V/hours.}$$

E.N.*	n	R^2	δV_{out} (V)	δb (V/hours)	%**	Best fit line
S-1	29	0.830	0.00769	1.845×10^{-5}	99.9	V_{out}=0.00010t+3.14890
S-2	160	0.991	0.00172	1.980×10^{-6}	99.9	V_{out}=0.00015t+2.17270

* E.N. is the experiment label defined in §3.4.
** % represents the percentages of confidence in the linear relationship between V_{out} and time t.

(3). ISFET Output as a Function of Temperature

E.N.	n	R^2	δV_{out} (V)	δb (V/°C)	%***	Best fit line
T-1	8	0.976	0.02272	0.00070	99.9	V_{out}= – 0.00459T+3.26355
T-2	13	0.983	0.00419	0.00012	99.9	V_{out}= – 0.00141T+3.25390

*** % represents the percentages of confidence in the linear relationship between V_{out} and temperature T.

(4) ISFET Output as a Function of Pressure

(A). For those experiments performed in unthermostated buffer solutions:

E.N.	n	R^2	δV_{out}(V)	δb(V/MPa)	%*	Best fit line
P-1	14	0.988	0.00078	0.00002	99.9	V_{out}= – 0.00028P+2.51940
P-2	10	0.971	0.00153	0.00005	99.9	V_{out}= – 0.00034P+2.61836
P-3	10	0.847	0.00273	0.00009	99.9	V_{out}= – 0.00027P+2.66397
P-4	10	0.968	0.00138	0.00004	99.9	V_{out}= – 0.00028P+2.72272
P-5	10	0.683	0.00427	0.00013	99.0	V_{out}= – 0.00024P+2.63516
P-6	10	0.941	0.00104	0.00004	99.9	V_{out}= – 0.00017P+2.68909
P-7	10	0.681	0.00455	0.00014	99.0	V_{out}= – 0.00026P+2.74772
P-8	10	0.703	0.00242	0.00006	99.0	V_{out}= – 0.00012P+2.68798

(B). For the experiments taken in thermostated buffer solutions:

E.N.	n	R^2	δV_{out}(v)	δb(v/MPa)	%*	Best fit line
PT-1	11	0.964	0.00390	0.00011	99.9	V_{out}= – 0.00077P+3.25249
PT-2	11	0.877	0.00520	0.00014	99.9	V_{out}= – 0.00052P+3.16325
PT-3	11	0.856	0.00486	0.00014	99.9	V_{out}= – 0.00045P+3.08956
PT-4	11	0.938	0.00379	0.00011	99.9	V_{out}= – 0.00057P+3.05324
PT-5	7	0.673	0.01642	0.00053	95.0	V_{out}= – 0.00069P+2.69909
PT-6	6	0.915	0.00717	0.00024	98.0	V_{out}= – 0.00061P+2.66953

* % represents the percentages of confidence in the linear relationships between V_{out} and pressure P.

CHAPTER 4. CONCLUSIONS

§4.1. Conclusions

1. The Relationship between V_{out} and pH

The ISFET Output in Figure 3.7, is equal to V_g.

From Equation 15 in Chapter 2, when I_D is a constant, the relationship between V_g and α_2^i is

$$V_g \propto -\frac{RT}{Z^i F} \ln \alpha_2^i .$$

According to [25], $\alpha_2^i = f[H^+]$, therefore,

$$V_{out}=V_g \propto -\ln[H^+] = -\frac{\log[H^+]}{\log e},$$

hence, $V_{out} \propto$ pH. So, theoretically speaking, there is a linear relationship between V_{out} and pH value.

Our experimental results (Table 13 and Figure 3.28-33) support this expectation. We are 99% confident that the relationship between V_{out} and pH value is linear from the experiment.

2. The Relationship between V_{out} and Temperature

According to §3.5 and Figure 3.12 and 3.13, the linear relationship between V_{out} and the temperature is over 99.9% sure. Furthermore, the data are over 97% represented by their best fit lines, we can therefore conclude that there is a linear relationship between V_{out} and the temperature from 25°C to 60°C.

The slopes of the best fit lines are –4.6(mv/°C) and –1.4(mv/°C) (Figure

3.12 and 3.13). They are relatively small, comparing to those of V_{out} vs pH curves (about 40(mv/pH) in Figure 3.28-3.33). Thus, we can conclude that the indicated pH value decreases slowly with a increasing temperature.

During these experiments, the ISFETs we had failed at a temperature around 60°C. We suspect that this was caused by thermal expansion which separated drain and/or source leads from the ISFET. Although these sets of data have shown good linear functions, further experiments are needed to support the conclusion and extend it to a higher temperature.

3. The Relationship between V_{out} and Pressure

Using the results from experiments P-1 to P-8, as shown in Table 5-8 and Figure 3.14-3.21, we can draw the conclusion that the relationship between V_{out} and the pressure on the solution is a linear function with a small slope, around –0.2 mv/MPa,from 101 kPa to 40MPa. This conclusion is further supported by the results from the experiments performed under several fixed temperatures as shown in Figure 3.22-3.27 (the slope is about –0.5 mv/MPa under this conditions).

An increase in pressure results in a small decrease in the indicated pH. The linear relations of pH with pressure or temperature as indicated pH provide the basis upon which practical instruments can be designed to give corrected values of pH under various conditions.

4. The Stability of V_{out}

From both of two stability tests, we are 99.9% confident that V_{out} changes slowly as a function of time. However, the second stability test (over 2,000 hours) indicates a more complicated relationship between V_{out} and time. Rather than a linear function, the trend of V_{out} can be more precisely

predicted by adding a very small second order term:

$$V_{out} = -1.95185\times10^{-8}t^2+0.00019t+2.15961.$$

According to Figure 3.39, the coefficient of correlation $R \propto 1$. So, the relationship between V_{out} and time can be considered to be linear in a short time period, but for a long term measurement, this relationship should be modified by using a polynomial equation.

§4.2. Suggestions for Improvements in Future Experiments

In the future, experiments should focus on the operation of ISFETs at higher temperatures. If possible, ISFETs with different encapsulants and contact binding procedures should be considered and tested as a function of temperature.

The satisfactory performance of the ISFETs as indicators of pH at the pressures found in geothermal/geopressured reservoirs has been demonstrated. It remains to be seen, however, if the ISFETs can function at temperature to 150°C.

Experiment S-1, 01/09/90	
Time (hours)	FET Output (v)
0.000	3.14906
8.085	3.14868
16.026	3.14841
32.101	3.15667
40.123	3.14246
48.062	3.15232
56.030	3.15380
64.101	3.15447
72.066	3.15660
88.324	3.15208
96.124	3.15913
103.594	3.16471
111.582	3.16036
119.599	3.16215
127.589	3.16253
135.621	3.15378
151.947	3.16532
159.581	3.16507
167.502	3.16595
175.468	3.16742
183.548	3.16888
191.538	3.16918
199.379	3.17056
207.608	3.17026
215.514	3.17495
223.502	3.17479
231.567	3.17108
239.531	3.16520
240.517	3.17187

Table 1. Stability Test of ISFET 3
pH=4.05; Temperature=25°C

Experiment S-2; pH=5.29; ISFET Output: volts; 12/18/90-03/13/91									
Time (hours)	ISFET Output	Time (hours)	ISFET Output	Time (hours)	ISFET Output	Time (hours)	ISFET Output	Time (hours)	ISFET Output
0.00	2.170	381.78	2.219	764.95	2.299	1149.12	2.362	1649.12	2.426
7.48	2.179	392.87	2.223	772.62	2.301	1157.12	2.361	1662.12	2.430
19.73	2.182	404.62	2.227	788.28	2.302	1177.12	2.366	1673.12	2.432
31.68	2.182	415.63	2.229	799.62	2.305	1185.62	2.367	1686.12	2.433
43.62	2.183	429.70	2.231	811.62	2.308	1192.12	2.366	1703.12	2.432
55.53	2.185	438.78	2.232	823.95	2.311	1204.12	2.368	1710.12	2.435
67.78	2.186	453.62	2.235	833.95	2.312	1224.12	2.369	1714.12	2.435
79.62	2.185	463.95	2.237	844.95	2.315	1229.12	2.370	1726.12	2.436
91.80	2.187	475.95	2.239	863.62	2.318	1242.12	2.373	1739.12	2.438
103.62	2.189	487.95	2.242	869.78	2.318	1339.12	2.386	1755.12	2.441
115.78	2.190	499.63	2.244	886.62	2.322	1351.62	2.391	1770.12	2.442
127.70	2.196	512.62	2.247	893.62	2.323	1370.12	2.391	1782.12	2.444
140.08	2.197	526.78	2.249	906.28	2.326	1390.62	2.393	1794.12	2.447
152.72	2.194	536.95	2.252	920.87	2.328	1400.12	2.397	1806.12	2.445
163.47	2.191	548.95	2.254	932.12	2.330	1412.12	2.400	1810.12	2.445
174.87	2.187	560.37	2.256	942.12	2.333	1442.12	2.402	1823.12	2.446
189.87	2.190	574.37	2.259	957.12	2.335	1451.12	2.403	1834.12	2.450
198.70	2.192	584.97	2.261	966.12	2.335	1464.12	2.403	1849.12	2.449
214.37	2.195	598.12	2.263	980.12	2.336	1473.12	2.403	1860.12	2.452
225.30	2.198	608.95	2.266	989.12	2.334	1488.12	2.406	1872.12	2.450
237.28	2.199	622.95	2.267	1005.12	2.342	1496.62	2.407	1887.12	2.456
248.53	2.200	632.95	2.271	1013.12	2.340	1508.62	2.410	1901.12	2.455
262.05	2.202	646.12	2.273	1028.12	2.344	1520.12	2.411	1907.12	2.457
274.20	2.204	656.38	2.277	1037.12	2.345	1541.12	2.417	1920.12	2.459
285.78	2.205	670.37	2.278	1056.12	2.346	1547.12	2.415	1928.12	2.460
298.62	2.205	681.95	2.284	1064.12	2.348	1559.12	2.417	1944.12	2.462
309.78	2.207	693.95	2.282	1078.12	2.347	1571.12	2.418	1963.12	2.465
318.95	2.210	704.12	2.288	1086.12	2.350	1584.12	2.418	1974.12	2.466
333.95	2.208	717.03	2.289	1100.12	2.352	1595.12	2.424	1988.12	2.466
342.62	2.211	728.62	2.291	1110.12	2.356	1602.12	2.424	2000.12	2.466
357.37	2.214	740.62	2.294	1126.12	2.356	1613.12	2.425	2016.12	2.468
368.03	2.216	753.45	2.296	1135.12	2.360	1637.12	2.427	2042.12	2.469

Table 2. Stability Test of ISFET 3039; Temperature: 25°C; Pressure: 101 KPa

Experiment T-1; pH=4.05 01/29/90	
Temperature (°C)	ISFET Output (v)
25	3.136
30	3.142
35	3.110
40	3.072
45	3.052
50	3.036
55	3.011
60	2.988

Table 3. ISFET Output as a Function of Temperature. Using the pH Probe R Which was Provided by Chemfet Company; Pressure: 101 KPa

Experiment T-2, pH=5.26 10/17/90	
Temperature (°C)	ISFET Output (v)
25	3.217
27	3.214
31	3.212
33	3.208
35	3.207
38	3.201
41	3.196
43	3.192
45	3.190
48	3.185
51	3.178
54	3.180
55	3.177

Table 4. ISFET 3021 Output as a Function of Temperature. Pressure: 101 KPa

Experiment P-2 pH=5.26		Experiment P-3 pH=6.27		Experiment P-4 pH=7.29	
Pressure (MPa)	FET (v) Output	Pressure (MPa)	FET (v) Output	Pressure (MPa)	FET (v) Output
6.16	2.615	8.64	2.660	6.59	2.720
7.86	2.616	9.76	2.661	8.28	2.720
10.57	2.615	11.52	2.662	10.14	2.720
14.26	2.614	13.48	2.662	14.90	2.719
17.91	2.612	16.94	2.660	17.66	2.718
21.41	2.612	20.44	2.657	22.00	2.717
25.56	2.610	24.25	2.657	26.59	2.716
29.59	2.608	28.35	2.655	30.19	2.714
33.86	2.607	32.04	2.655	34.42	2.713
37.15	2.605	36.01	2.655	38.16	2.711

Table 6. ISFET 3041 Output as a Function of Pressure. Date: June 13, 1990

Experiment P-1; pH=6.84; 06/07/90	
Pressure (MPa)	FET (v) Output
0.21	2.519
7.25	2.517
7.43	2.517
8.57	2.517
9.44	2.517
10.94	2.517
13.54	2.516
15.99	2.515
19.68	2.514
23.50	2.513
27.19	2.512
30.87	2.511
34.83	2.509
37.84	2.509

Table 5. ISFET 3041 Output as a Function of Pressure. Temperature: 25°C

Experiment P-5 pH=5.26		Experiment P-6 pH=6.27		Experiment P-7 pH=7.29	
Pressure (MPa)	ISFET Output(v)	Pressure (MPa)	ISFET Output(v)	Pressure (MPa)	ISFET Output(v)
6.72	2.635	9.58	2.687	7.58	2.743
8.69	2.634	12.21	2.687	9.37	2.746
12.14	2.633	15.87	2.686	11.99	2.743
16.02	2.628	18.18	2.686	15.41	2.747
19.30	2.628	22.31	2.686	18.11	2.744
23.28	2.632	26.59	2.685	22.25	2.741
27.23	2.628	29.89	2.684	26.23	2.743
30.96	2.628	34.14	2.683	30.34	2.741
34.59	2.628	37.99	2.682	34.63	2.738
38.60	2.626			38.59	2.736

Table 7. ISFET 3041 Output as a Function of Pressure. Date: June 15, 1990

Experiment P-8 pH=6.27	
Pressure (MPa)	ISFET Output (v)
0.17	2.688
15.34	2.687
17.15	2.687
22.41	2.685
25.14	2.684
29.10	2.683
32.94	2.683
37.15	2.685
40.72	2.684
43.98	2.683

Table 8. ISFET 3049 Output as a Function of Pressure. Date: Aug. 15, 1990

Experiment PT-1 Temperature=40°C		Experiment PT-2 Temperature=50°C		Experiment PT-3 Temperature=60°C		Experiment PT-4 Temperature=70°C	
Pressure (MPa)	FET (v) Output	Pressure (MPa)	FET (v) Output	Pressure (MPa)	FET (v) Output	Pressure (MPa)	FET (v) Output
6.12	3.250	5.78	3.164	6.75	3.091	6.97	3.052
8.59	3.246	8.69	3.161	10.00	3.085	9.95	3.048
11.49	3.244	11.24	3.156	11.71	3.084	13.05	3.046
13.86	3.241	13.89	3.154	15.53	3.081	14.77	3.044
16.87	3.238	17.54	3.153	17.55	3.080	17.26	3.042
20.35	3.235	21.17	3.151	20.84	3.079	21.47	3.040
24.91	3.234	24.57	3.148	25.21	3.076	24.96	3.037
28.39	3.232	28.35	3.147	28.90	3.075	28.83	3.036
32.05	3.225	32.51	3.146	33.47	3.074	32.94	3.033
35.78	3.225	36.54	3.147	36.57	3.075	36.21	3.035
38.93	3.225	39.27	3.145	39.56	3.074	39.88	3.032

Table 9. ISFET 3041 Output as a Function of Pressure at Constant Temperatures
Date: July 6, 1990; pH=5.26

Experiment PT-5 Temperature=26°C		Experiment PT-6 Temperature=37°C	
Pressure (MPa)	FET (v) Output	Pressure (MPa)	FET (v) Output
0.17	2.710	0.23	2.670
7.65	2.686	8.32	2.666
10.34	2.688	14.08	2.658
17.59	2.685	20.84	2.655
20.94	2.682	29.93	2.655
27.76	2.681	35.87	2.646
38.00	2.677		

Table 10. ISFET 3049 Output as a Function of Pressure at Constant Temperatures
Date: Aug. 16, 1990; pH=6.27

P=13.6519V+7.0777	
Pressure (MPa)	Transducer Output (v)
0.10	0.524
6.94	1.026
13.77	1.527
20.61	2.029
27.44	2.530
34.28	3.031
41.12	3.529
47.95	4.033
54.79	4.533
61.62	5.032
68.46	5.530

Table 11. Calibration of the Pressure Transducer. Performed by M-TEC/RISE, INC. Temperature: 26°C; Date: Aug. 24, 1990

T=19.6004V+1.31792	
Temperature (°C)	Thermocouple Output (v)
37.30	1.807
41.90	2.057
45.80	2.251
50.49	2.501
54.87	2.780
60.15	3.030
65.75	3.307
69.30	3.502
75.30	3.779
80.50	4.030
86.30	4.280

Table 12. Calibration of the Thermocouple; Date: June 28, 1990; Voltage Measurement: Fluke Multimeter; Temperature Measurement: CMS Precision Thermometer

Dec. 18, 1990 17:23		Dec. 19, 1990 0:52		Dec. 19, 1990 13:07		Dec. 20, 1990 1:04		Dec. 20, 1990 13:00		Dec. 21, 1990 0:55	
pH	ISFET Output (v)	pH	ISFET Output (v)	pH	ISFET Output (v)	pH	ISFET Output (v)	pH	ISFET Output (v)	pH	ISFET Output (v)
5.29	2.170	5.29	2.179	5.29	2.182	5.29	2.182	5.29	2.183	5.29	2.186
7.29	2.270	7.29	2.277	7.29	2.268	7.29	2.273	7.29	2.276	7.29	2.276
9.05	2.355	9.05	2.359	9.05	2.347	9.05	2.357	9.05	2.360	9.05	2.359
10.60	2.393	10.60	2.397	10.60	2.391	10.60	2.393	10.60	2.395	10.60	2.394

Table 13. FET 3039 Output as a Function of pH Value; Temperature: 25 C; Pressure: 101Kpa

Probability of a Larger Value of R					
n-2	A=0.1	A=0.05	A=0.02	A=0.01	A=0.001
1	0.988	0.997	1.000	1.000	1.000
2	0.900	0.950	0.980	0.990	1.000
3	0.805	0.878	0.934	0.959	0.991
4	0.729	0.811	0.882	0.917	0.974
5	0.669	0.754	0.833	0.874	0.951
6	0.622	0.707	0.789	0.834	0.925
7	0.582	0.666	0.750	0.780	0.898
8	0.549	0.632	0.716	0.765	0.872
9	0.521	0.602	0.685	0.735	0.847
10	0.497	0.576	0.658	0.708	0.823
12	0.458	0.532	0.612	0.661	0.780
14	0.426	0.497	0.574	0.623	0.742
16	0.400	0.468	0.542	0.590	0.708
18	0.378	0.444	0.516	0.561	0.679
20	0.360	0.423	0.492	0.537	0.652
25	0.323	0.381	0.445	0.487	0.597
30	0.296	0.349	0.409	0.449	0.554
35	0.275	0.325	0.381	0.418	0.519
40	0.257	0.304	0.358	0.393	0.490
45	0.243	0.288	0.338	0.372	0.465
50	0.231	0.273	0.322	0.354	0.443

Table 14. Confidence Range of Correlation Coefficient R
Refer to Reference 27

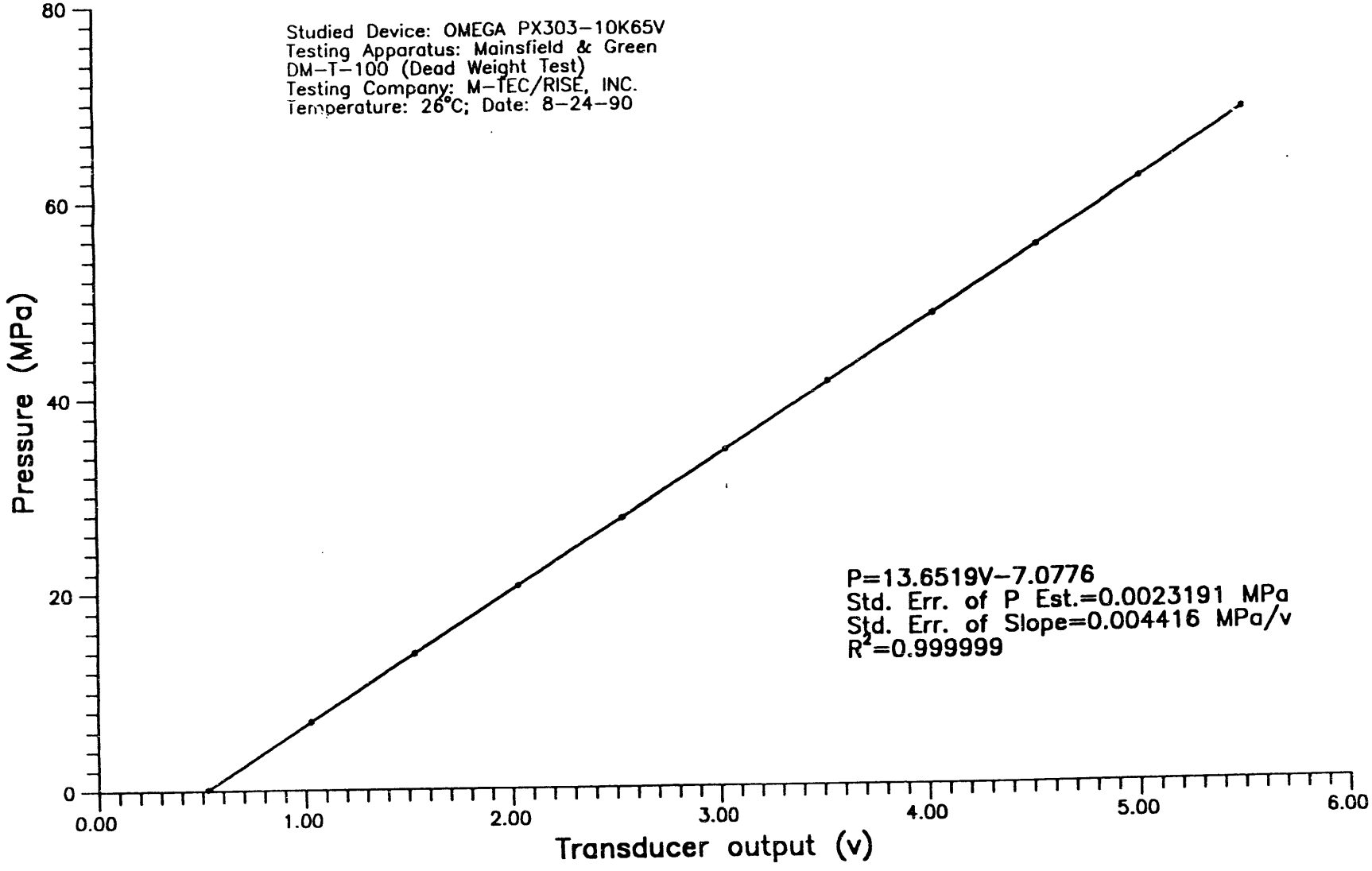

Figrue 3.8 Calibration of the Pressure Transducer

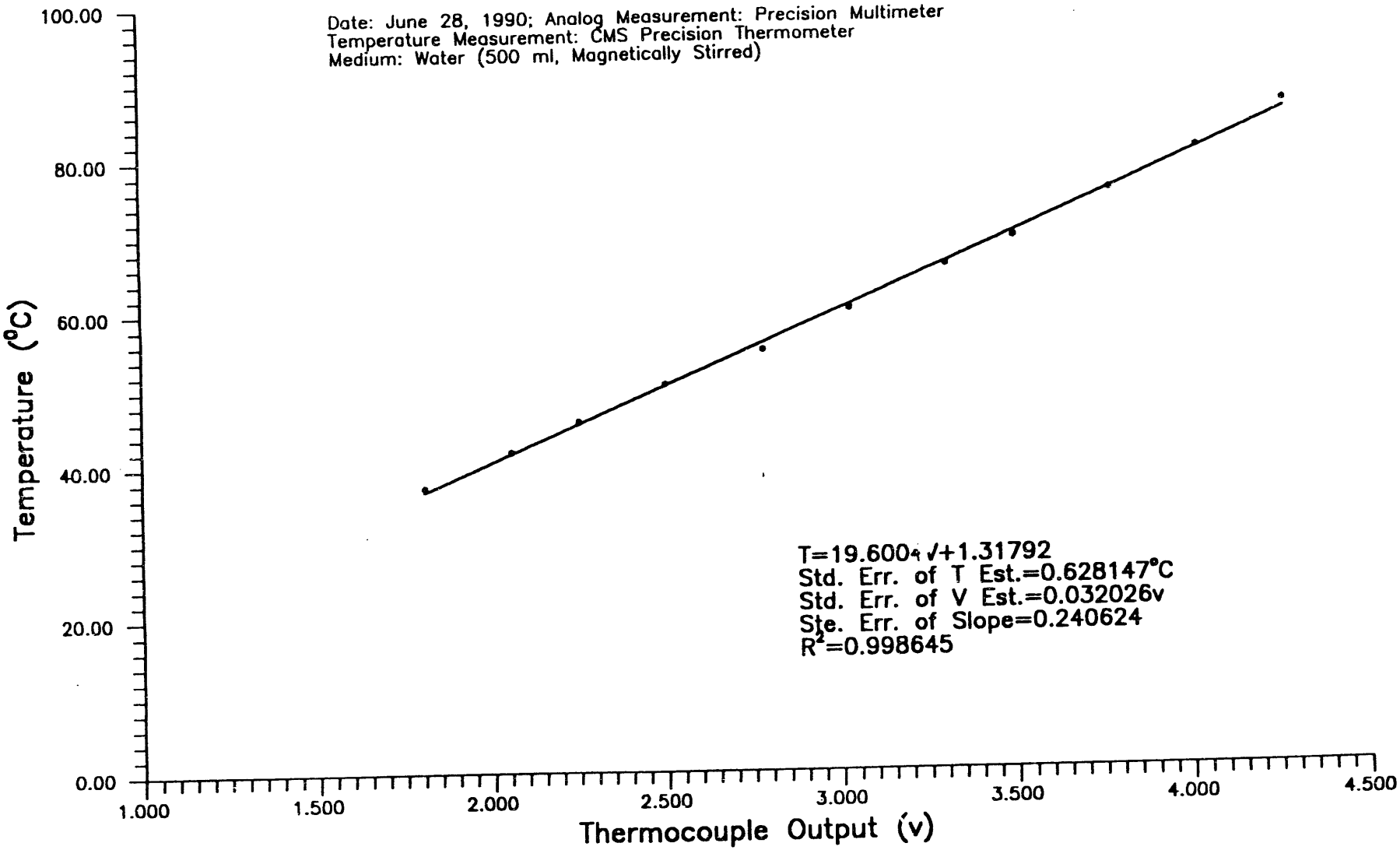

Figure 3.9 Calibration of the Thermocouple

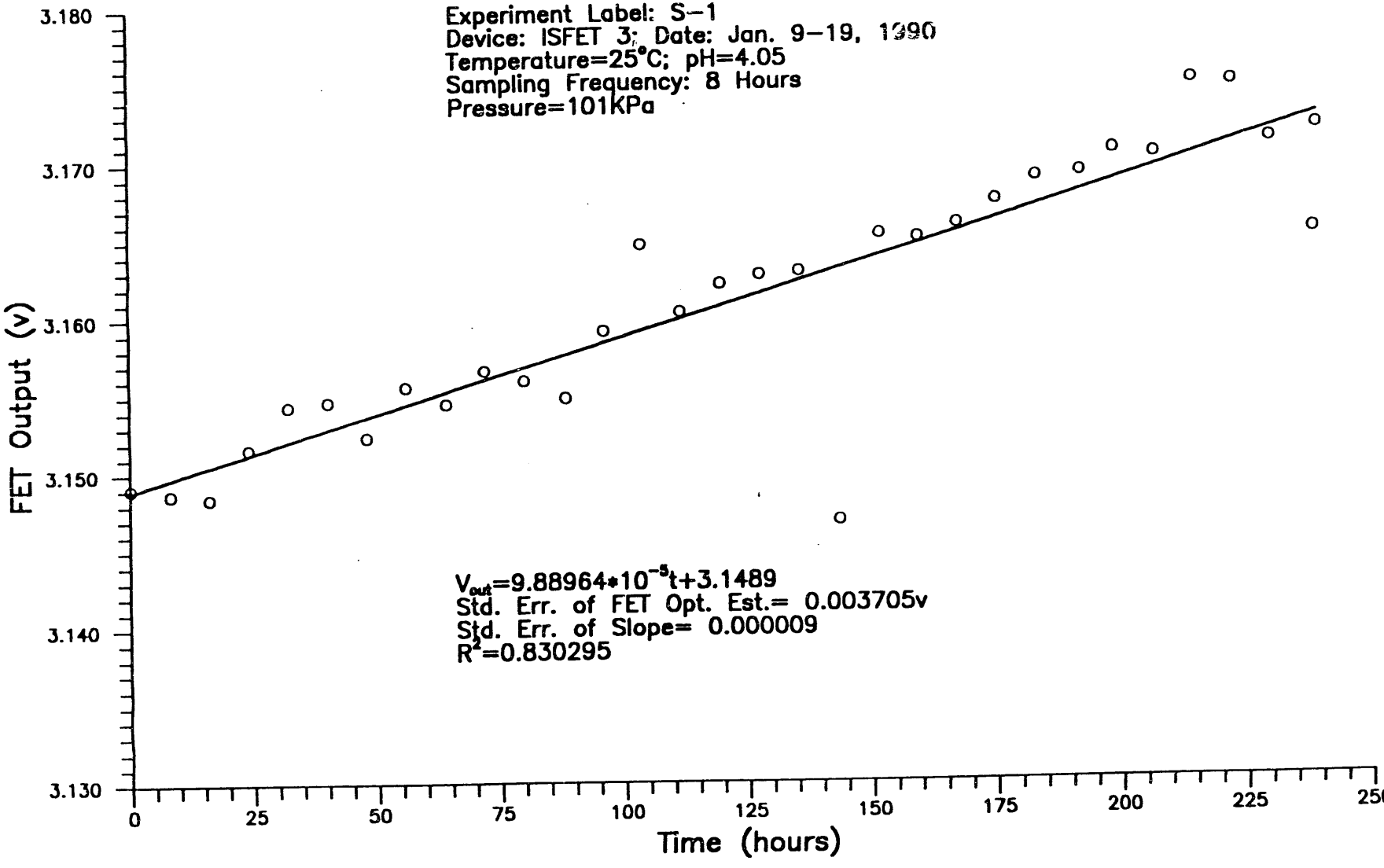

Figure 3.10 Stability Test of ISFET in pH 4.05 Buffered Solution

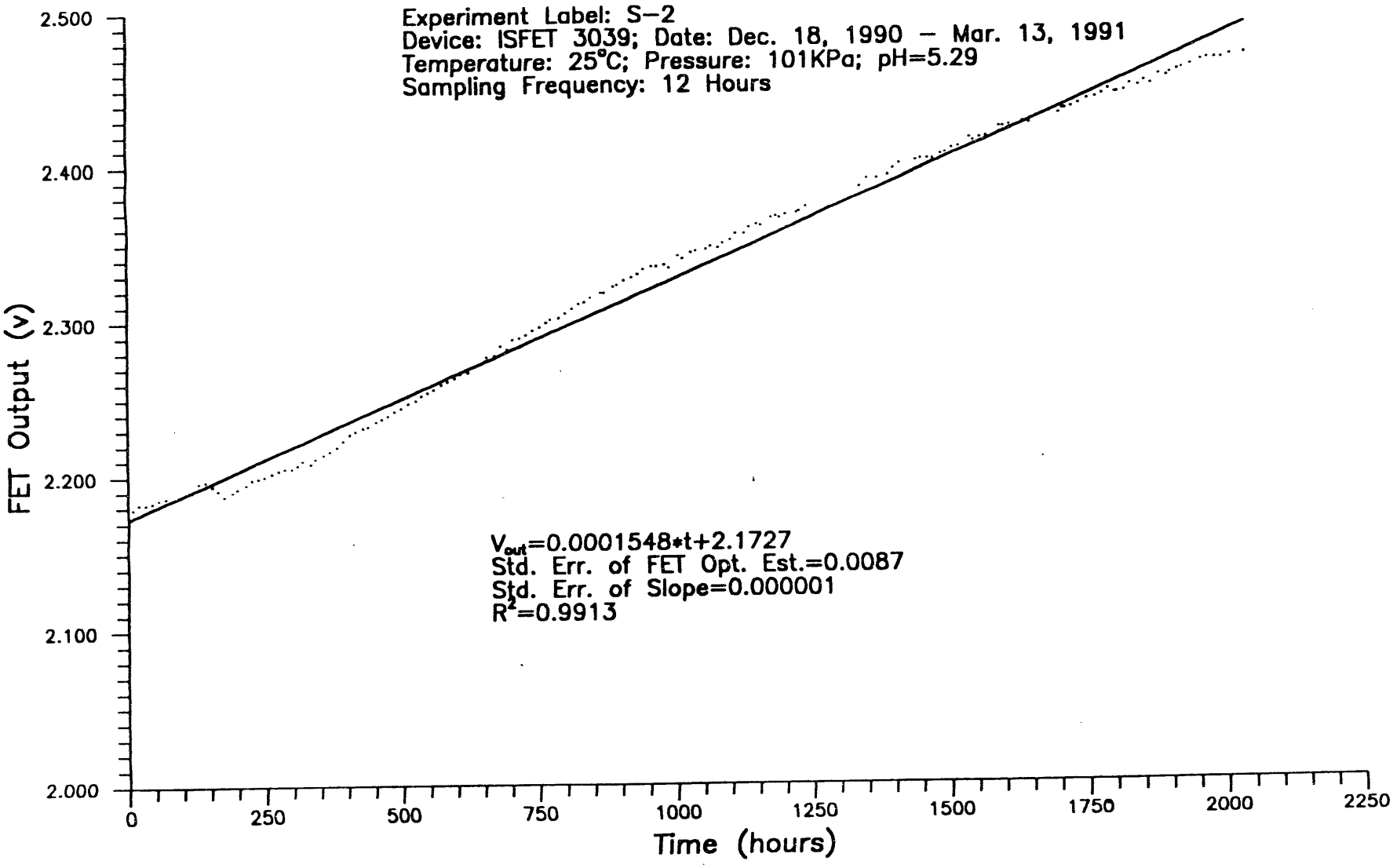

Figure 3.11 Stability Test of ISFET 3039 in pH 5.29 Buffered Solution

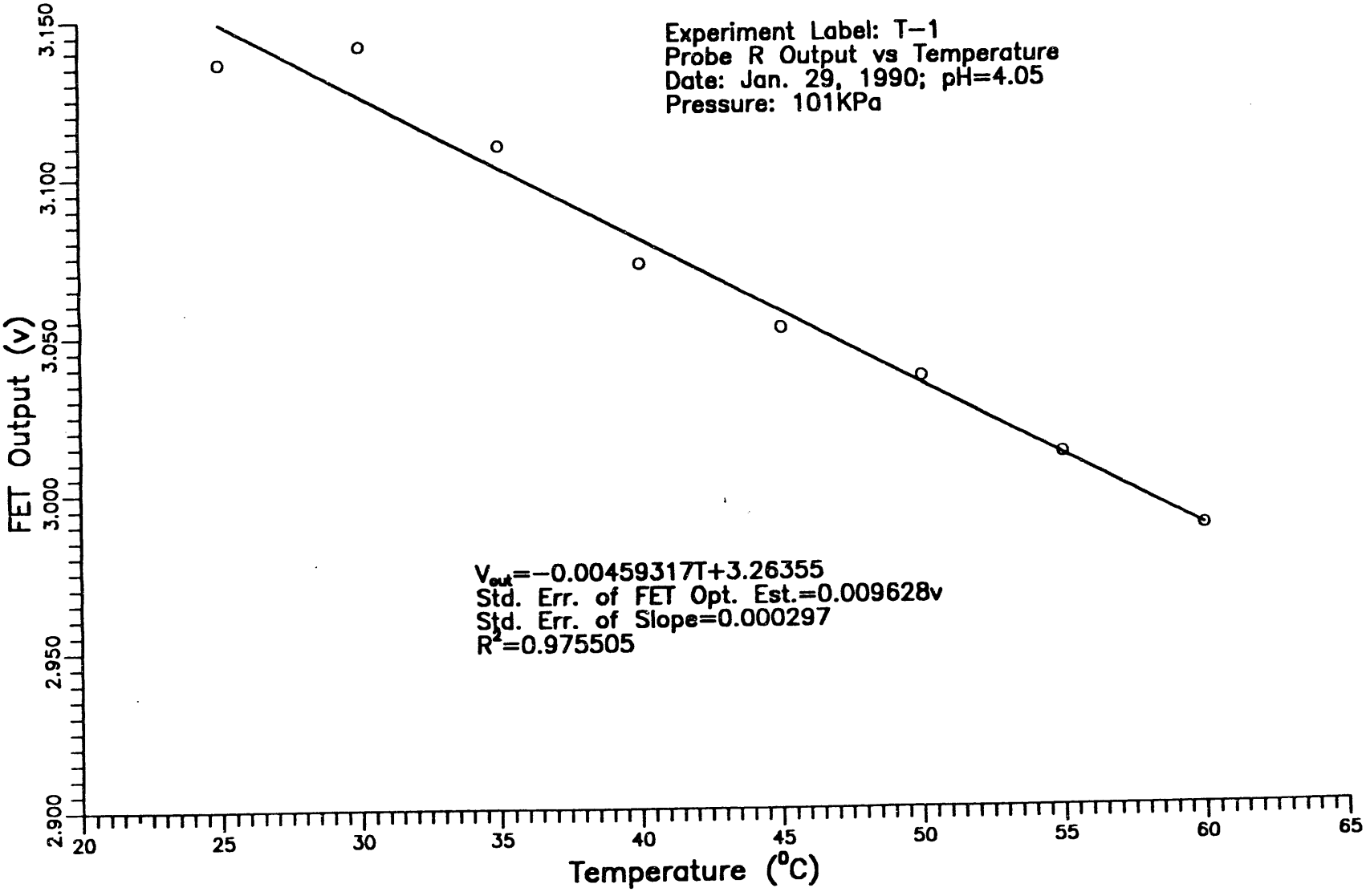

Figure 3.12 ISFET Output as a Function of Temperature

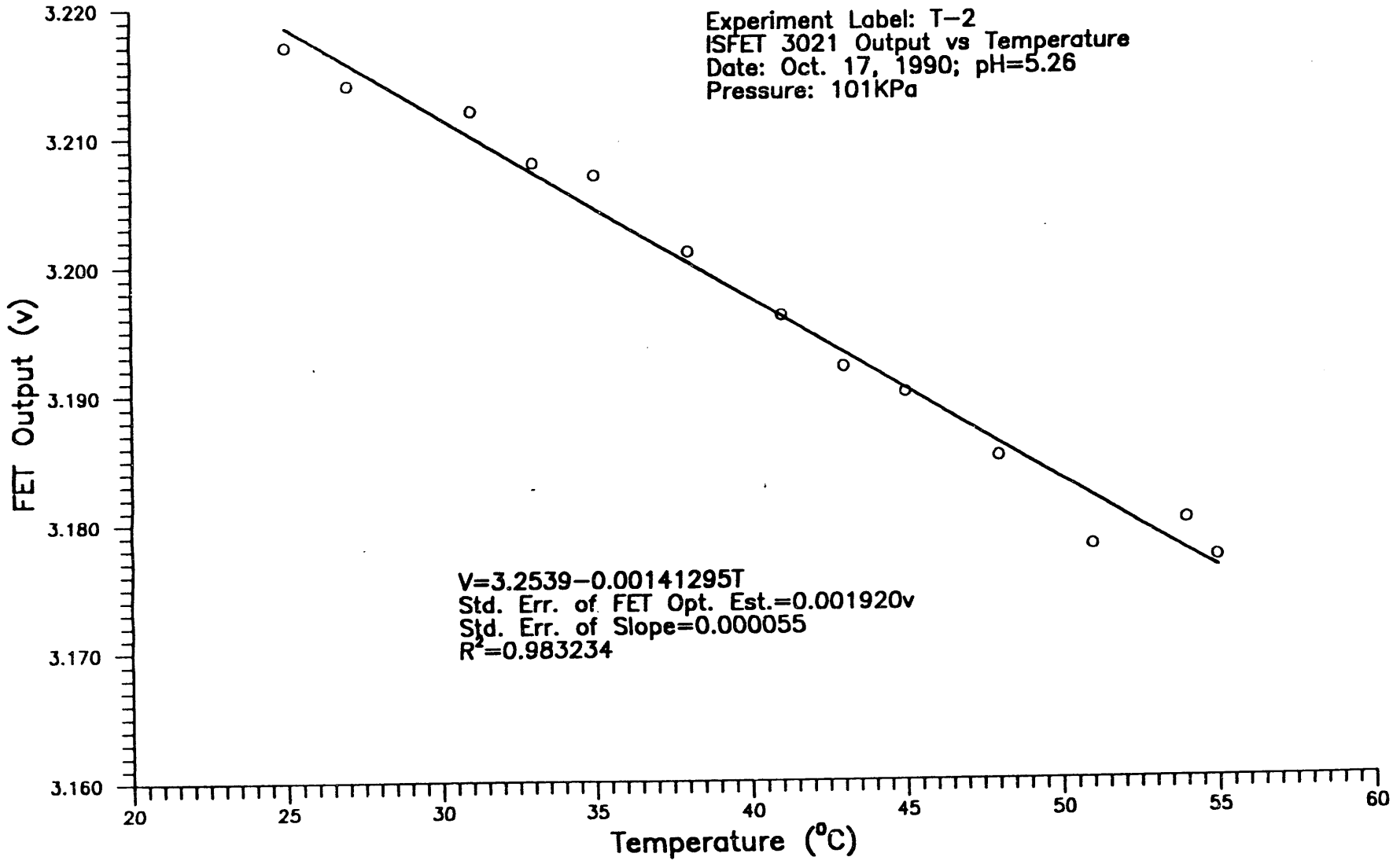

Figure 3.13 ISFET Output as a Function of Temperature

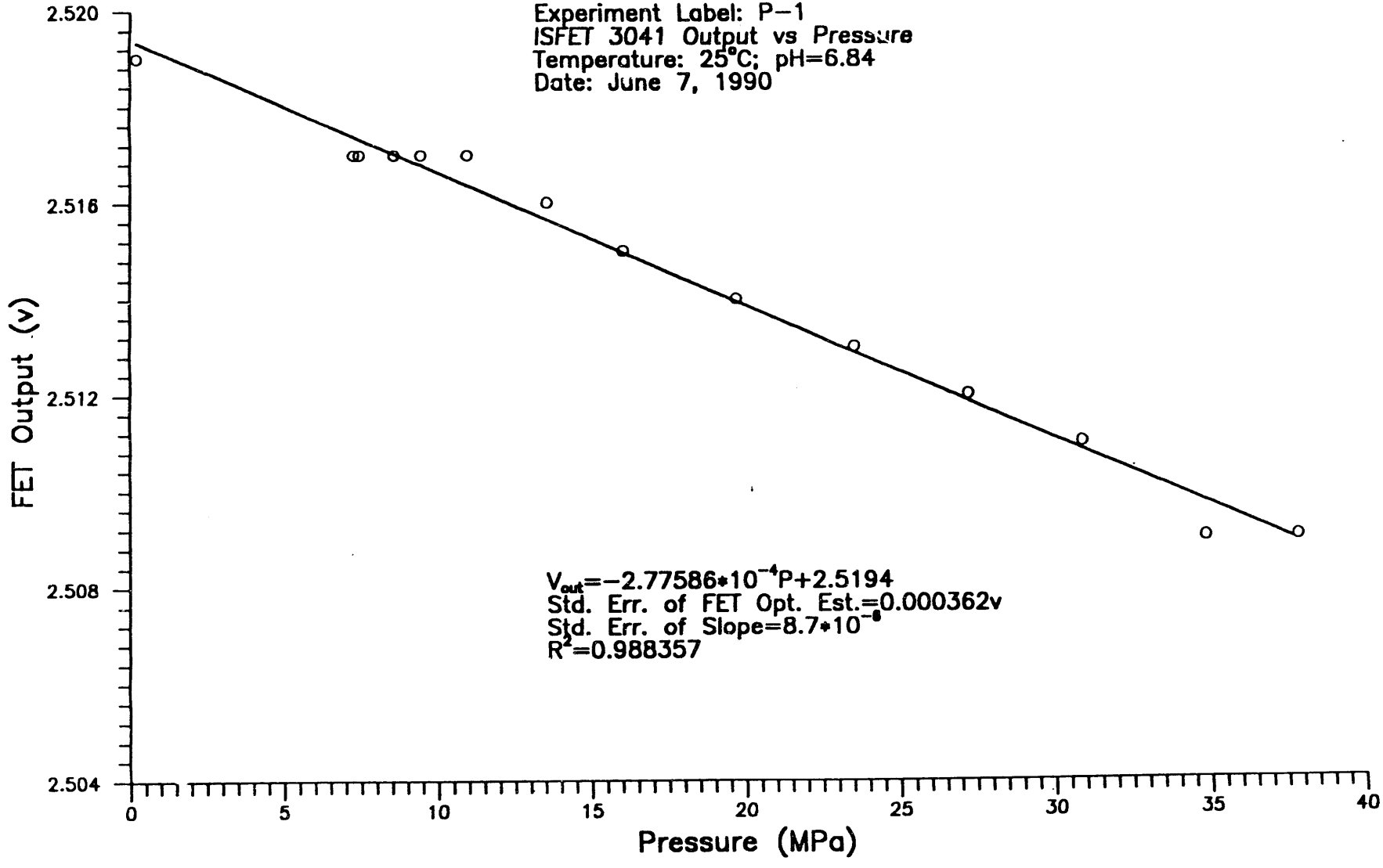

Figure 3.14 ISFET Output as a Function of Pressure

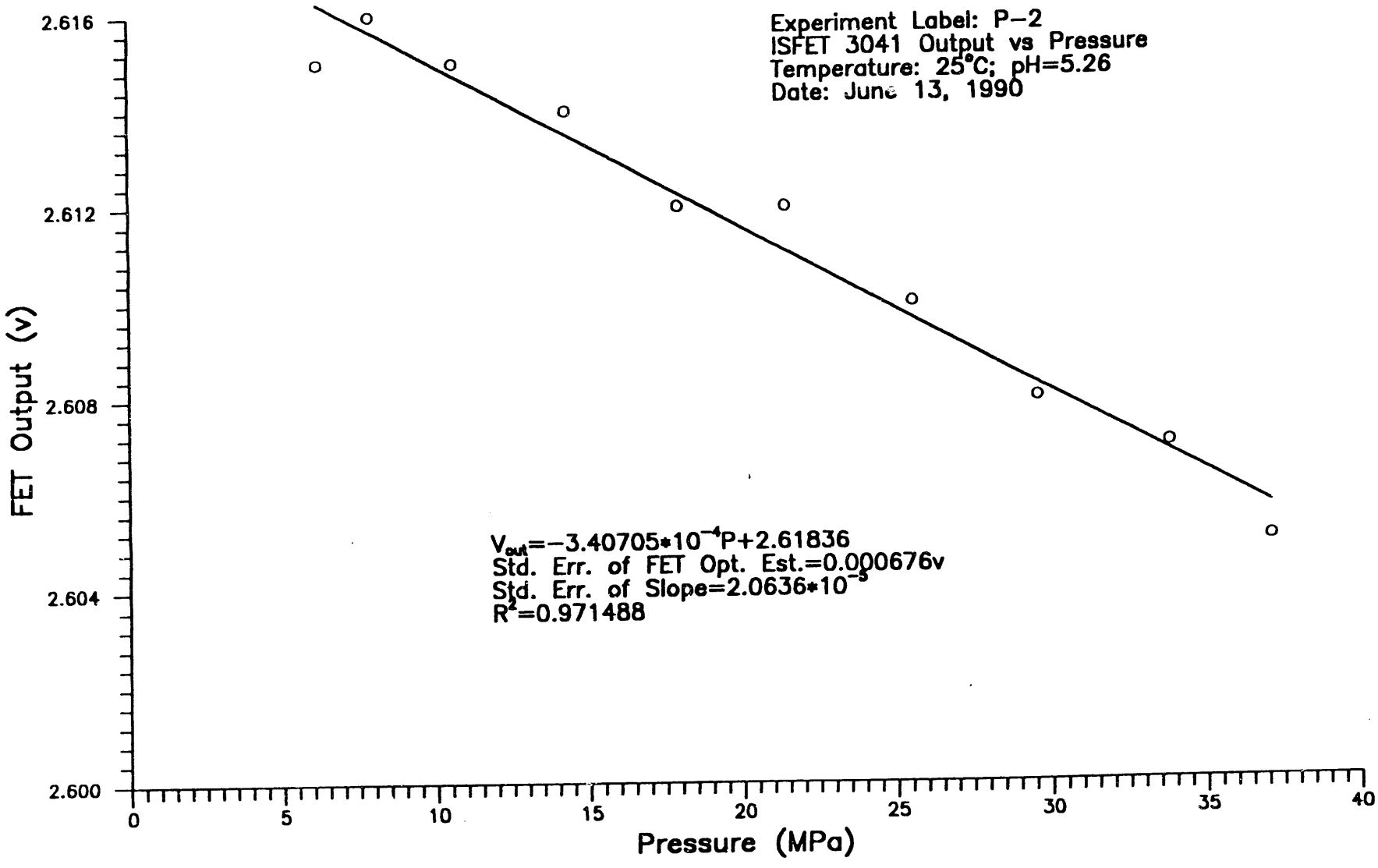

Figure 3.15 ISFET Output as a Function of Pressure

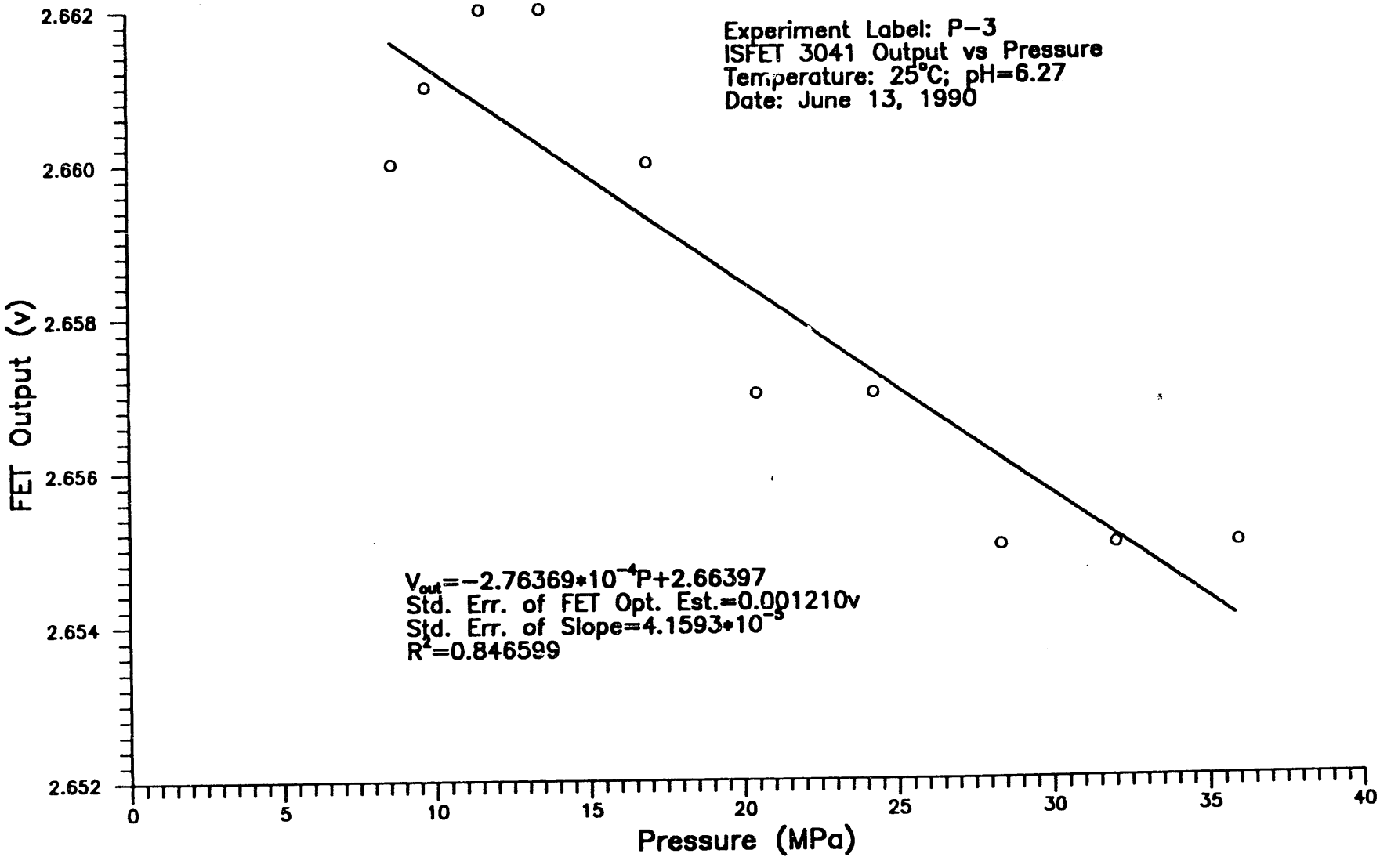

Figure 3.16 ISFET Output as a Function of Pressure

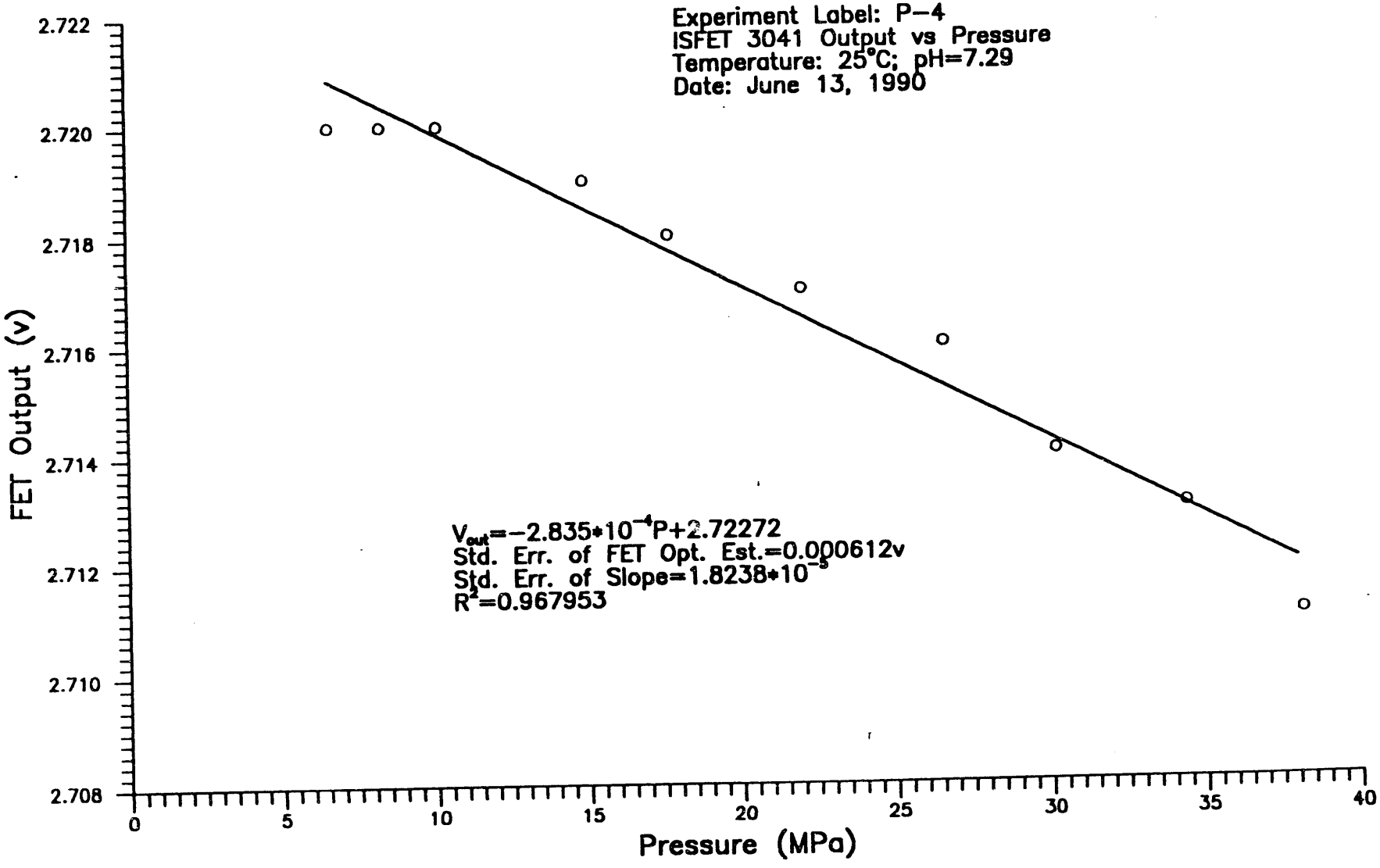

Figure 3.17 ISFET Output as a Function of Pressure

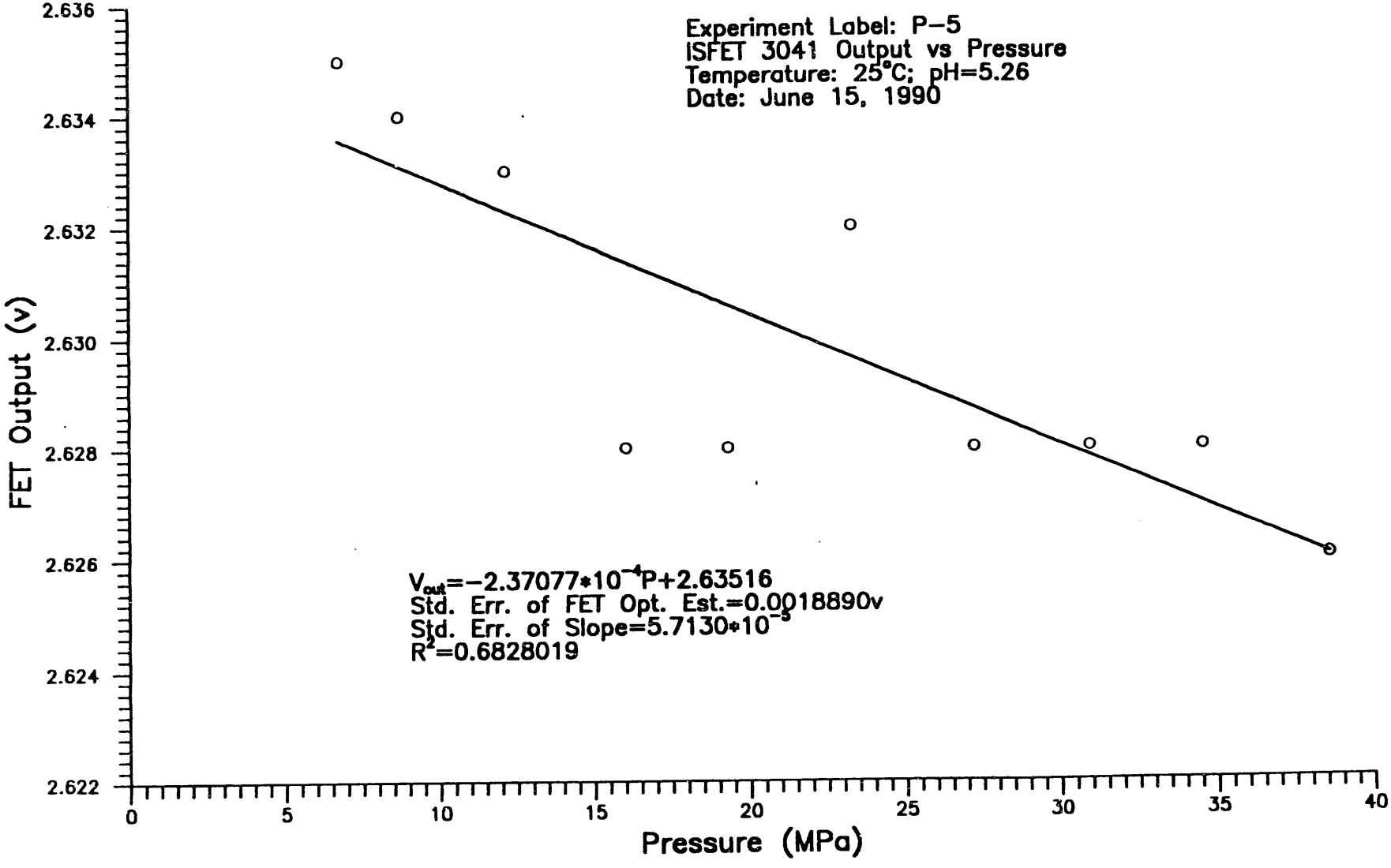

Figure 3.18 ISFET Output as a Function of Pressure

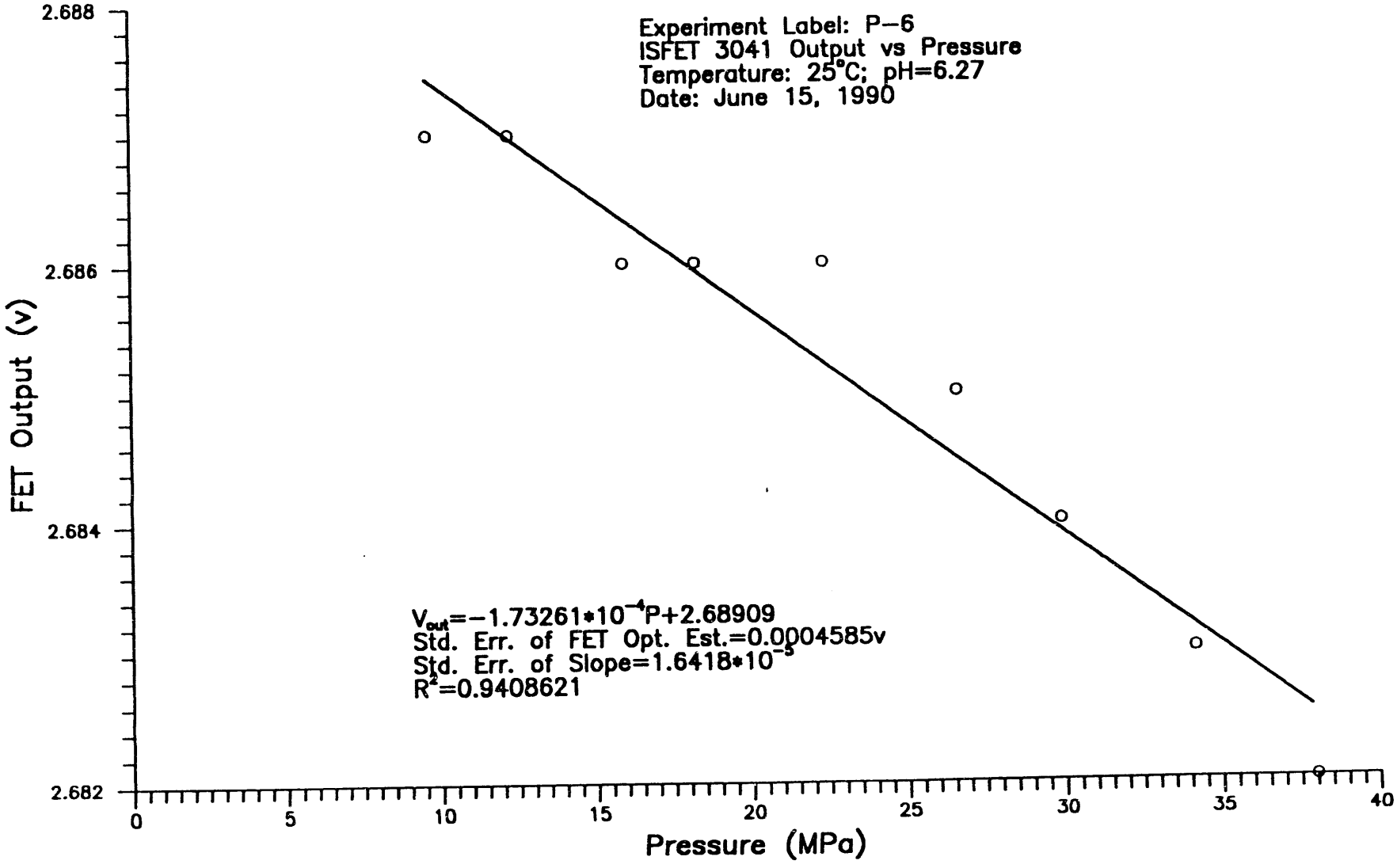

Figure 3.19 ISFET Output as a Function of Pressure

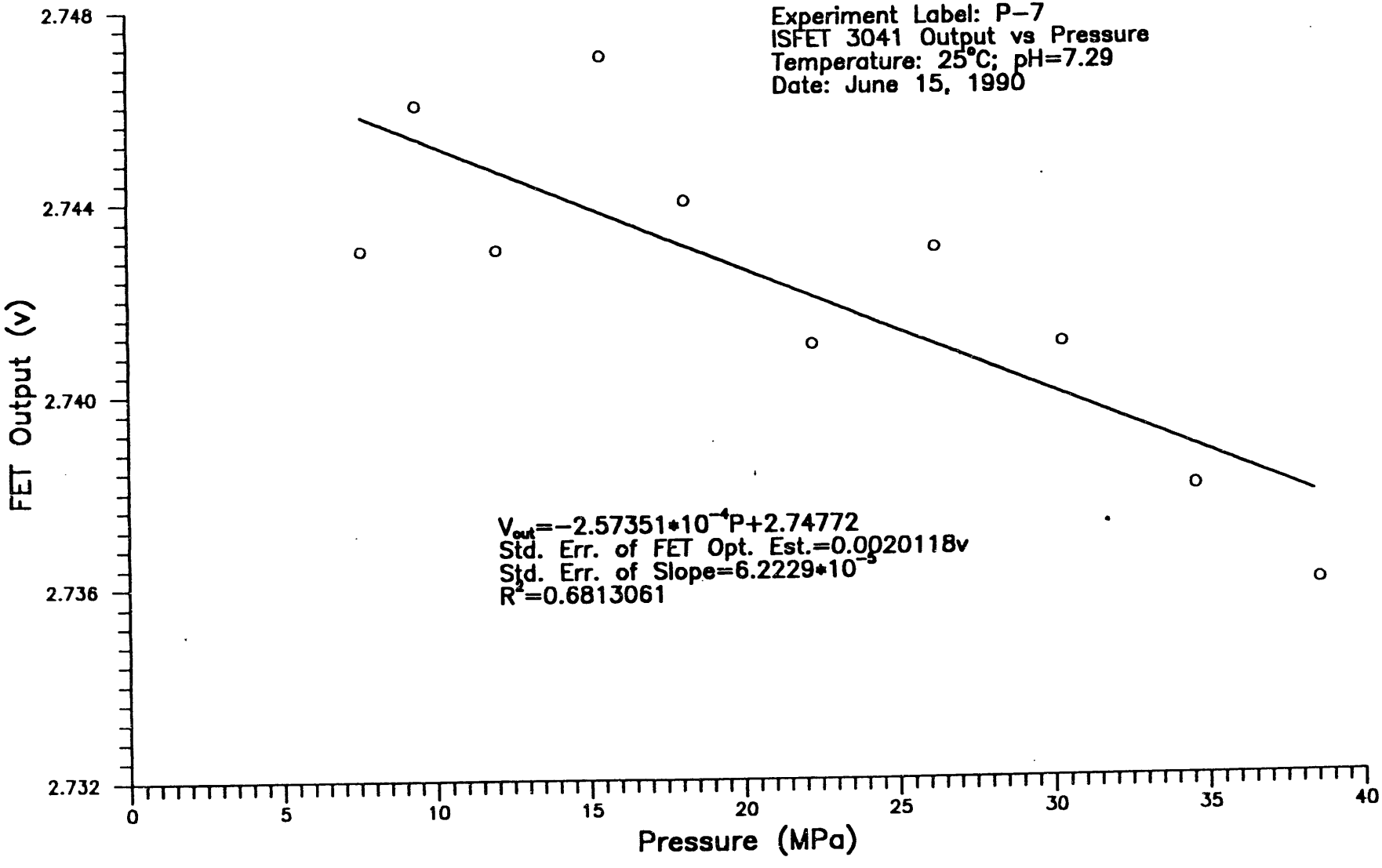

Figure 3.20 ISFET Output as a Function of Pressure

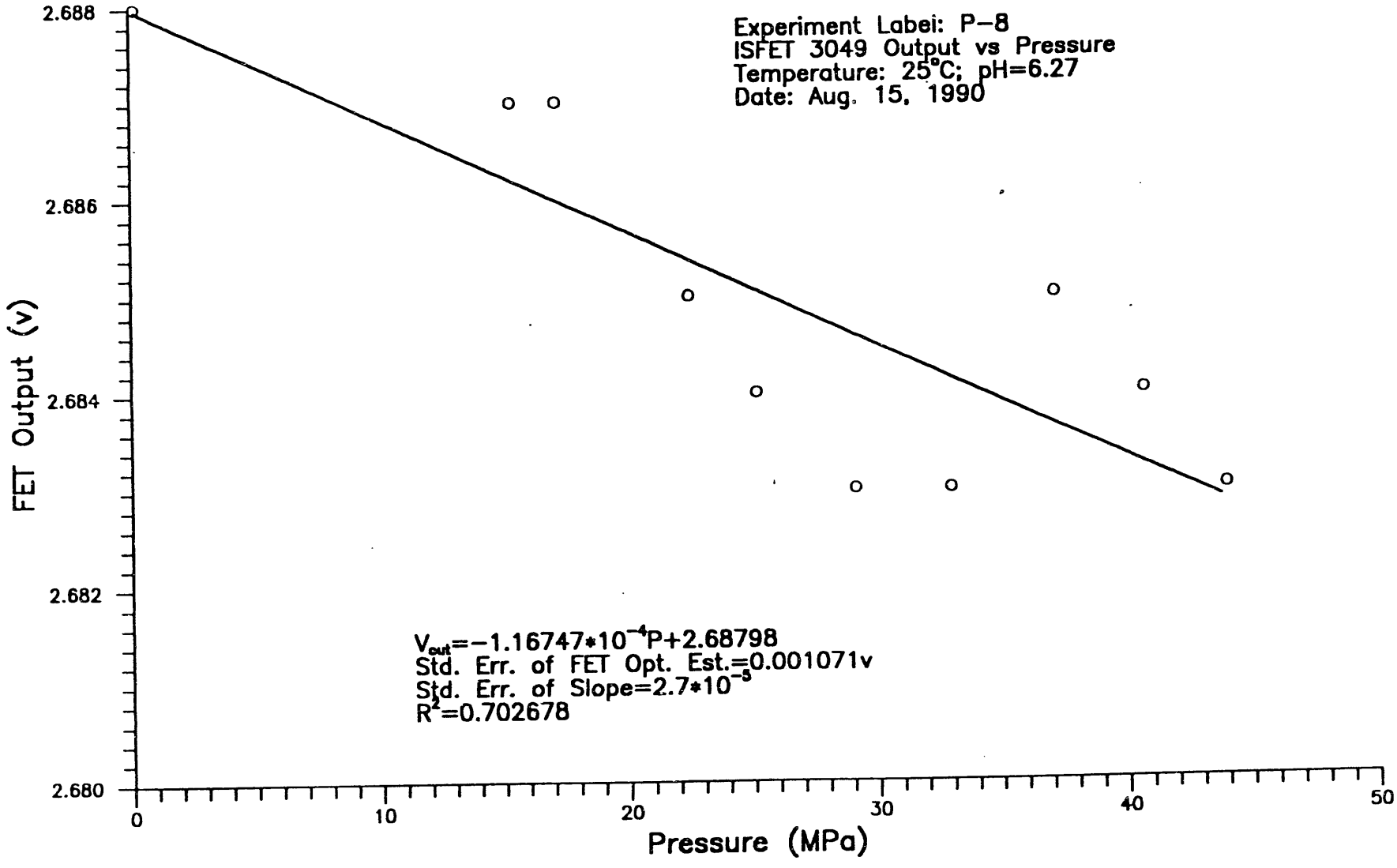

Figure 3.21 ISFET Output as a Function of Pressure

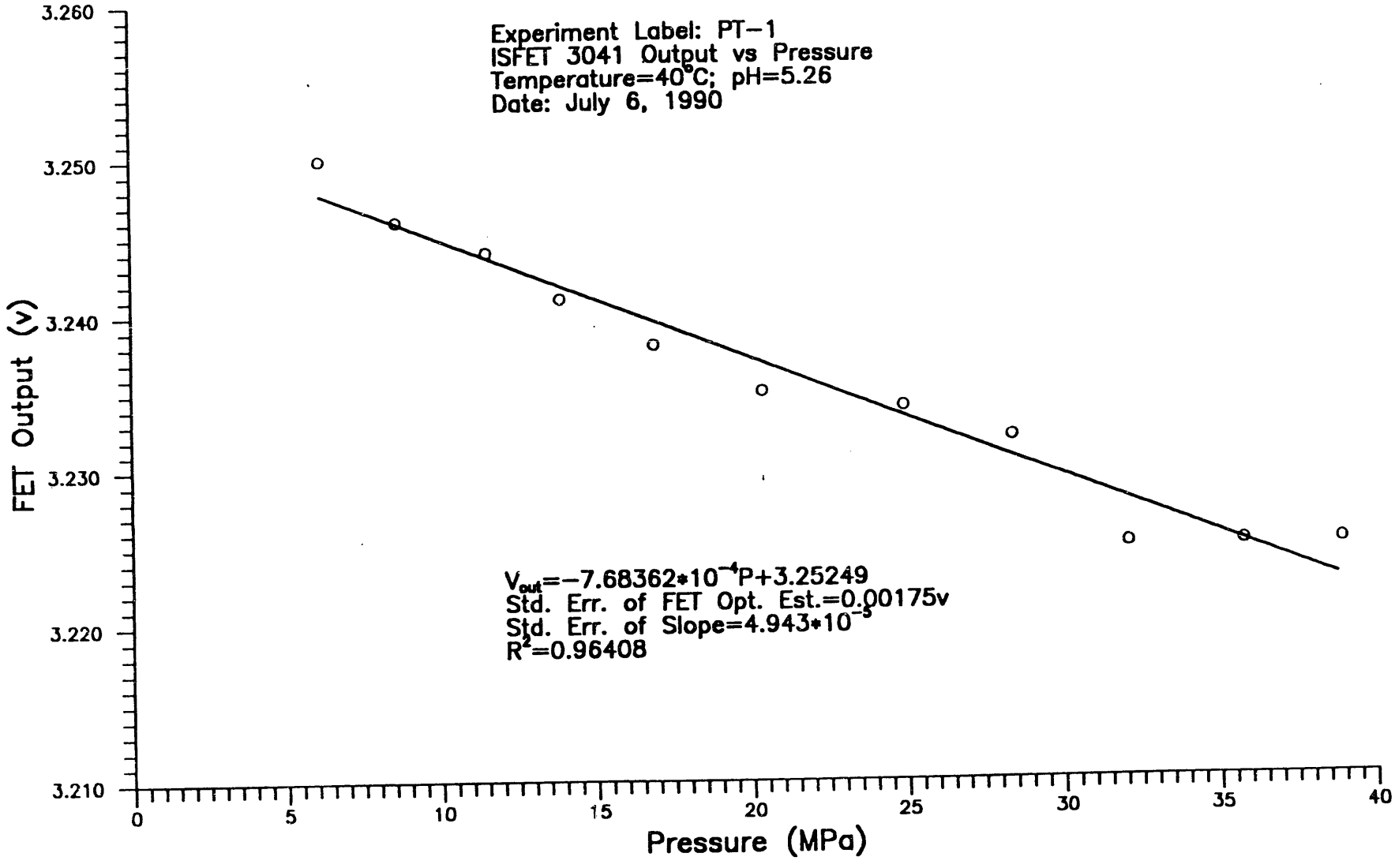

Figure 3.22 ISFET Output as a Function of Pressure at 40°C

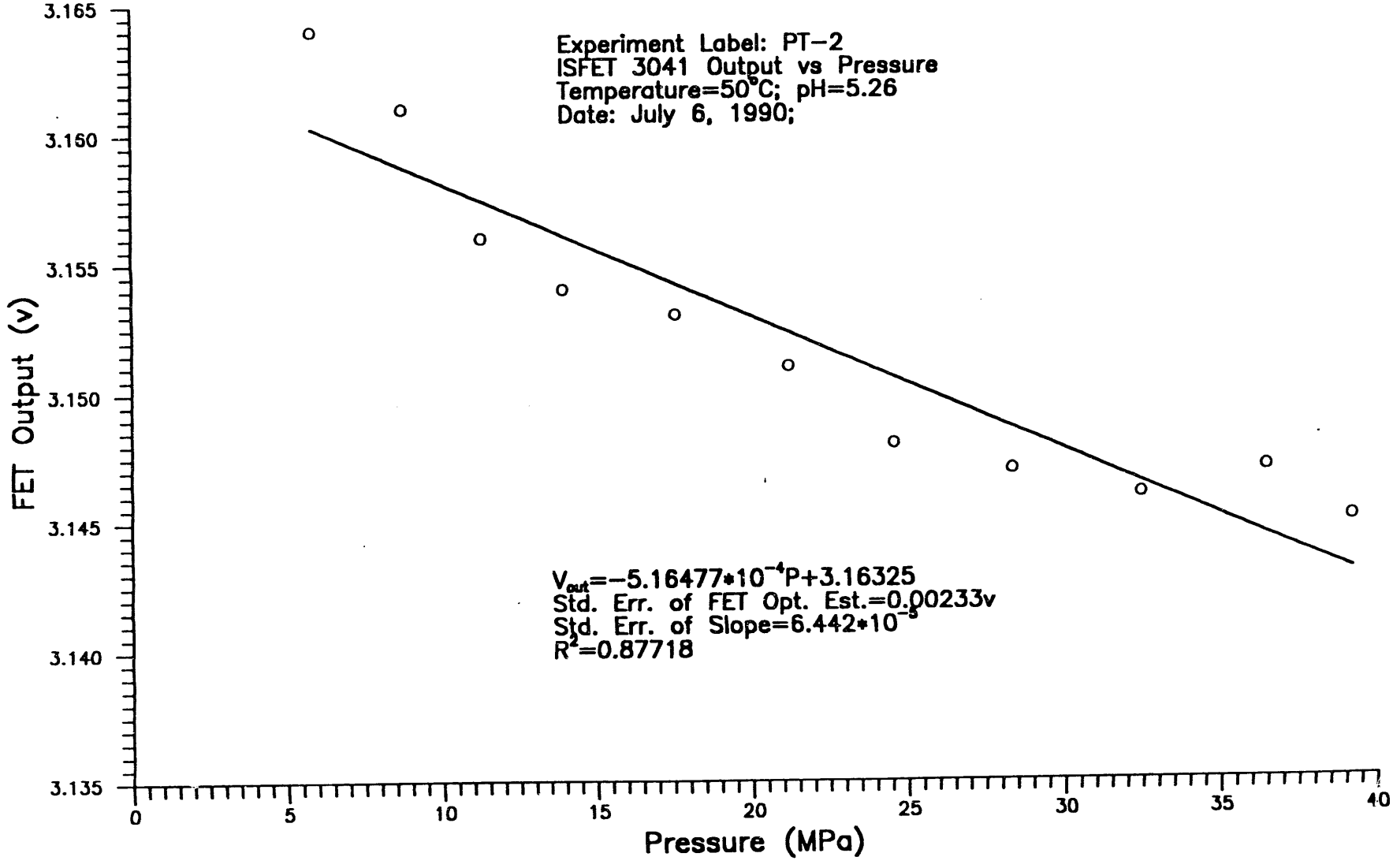

Figure 3.23 ISFET Output as a Function of Pressure at 50°C

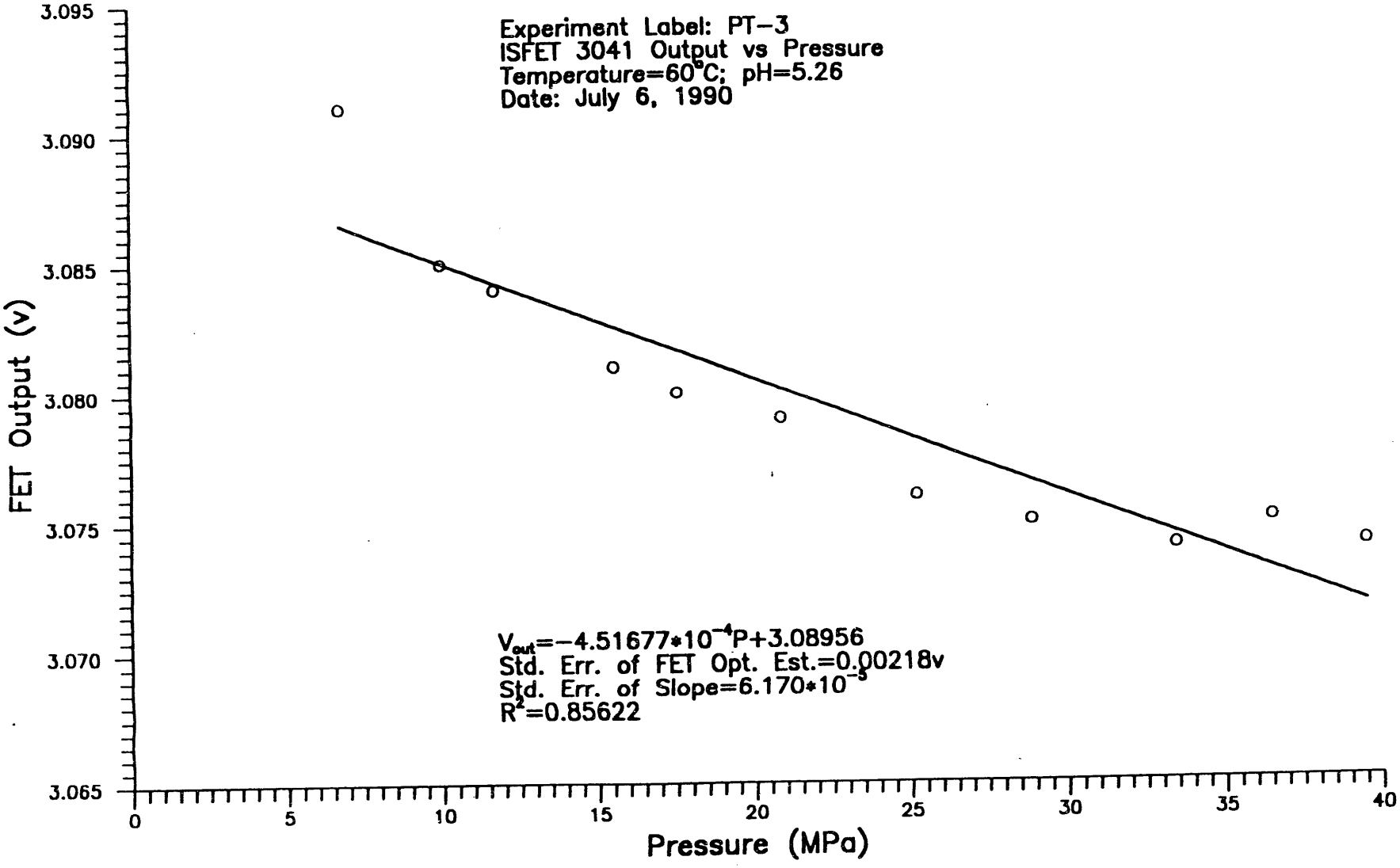

Figure 3.24 ISFET Output as a Function of Pressure at 60°C

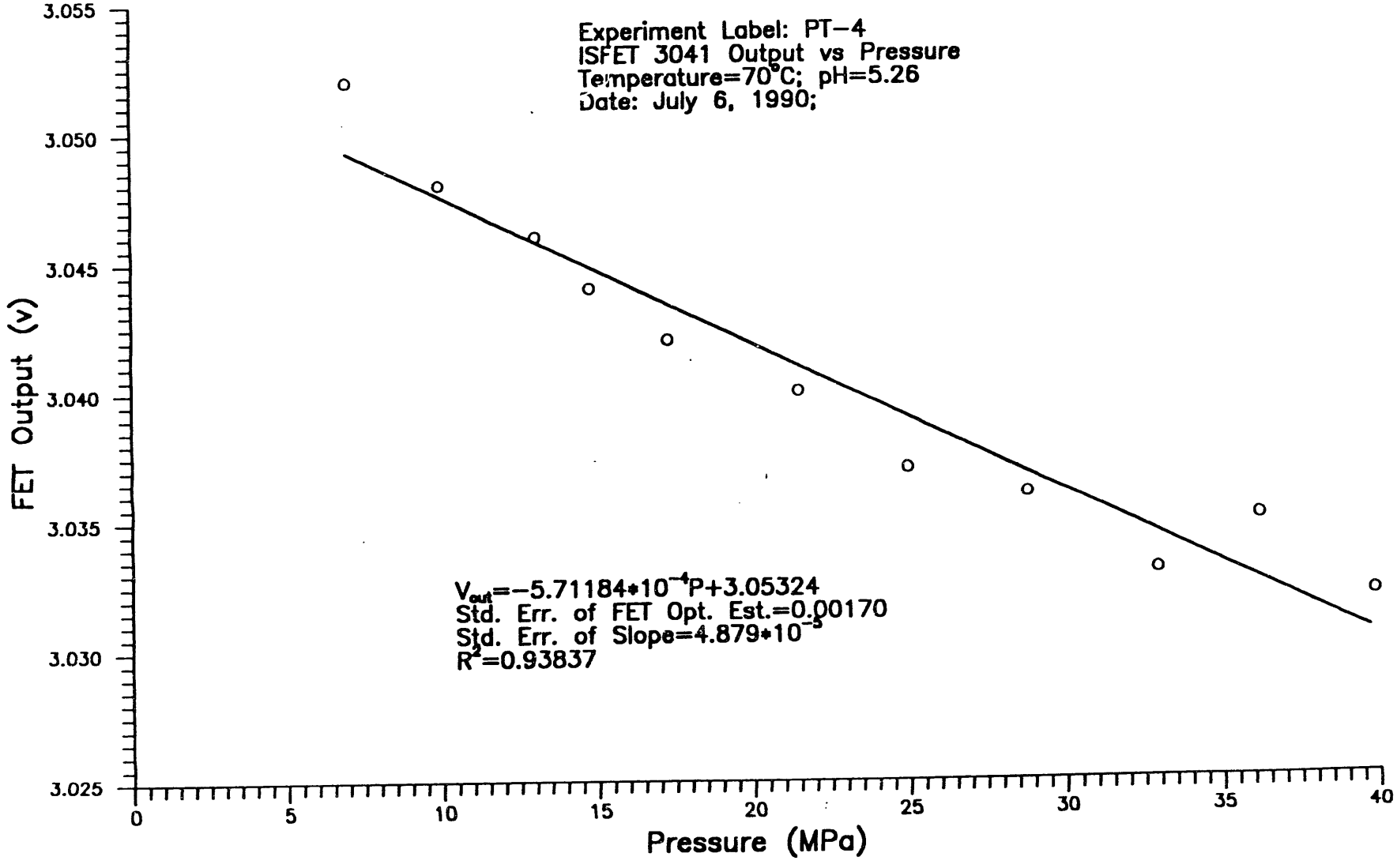

Figure 3.25 ISFET Output as a Function of Pressure at 70°C

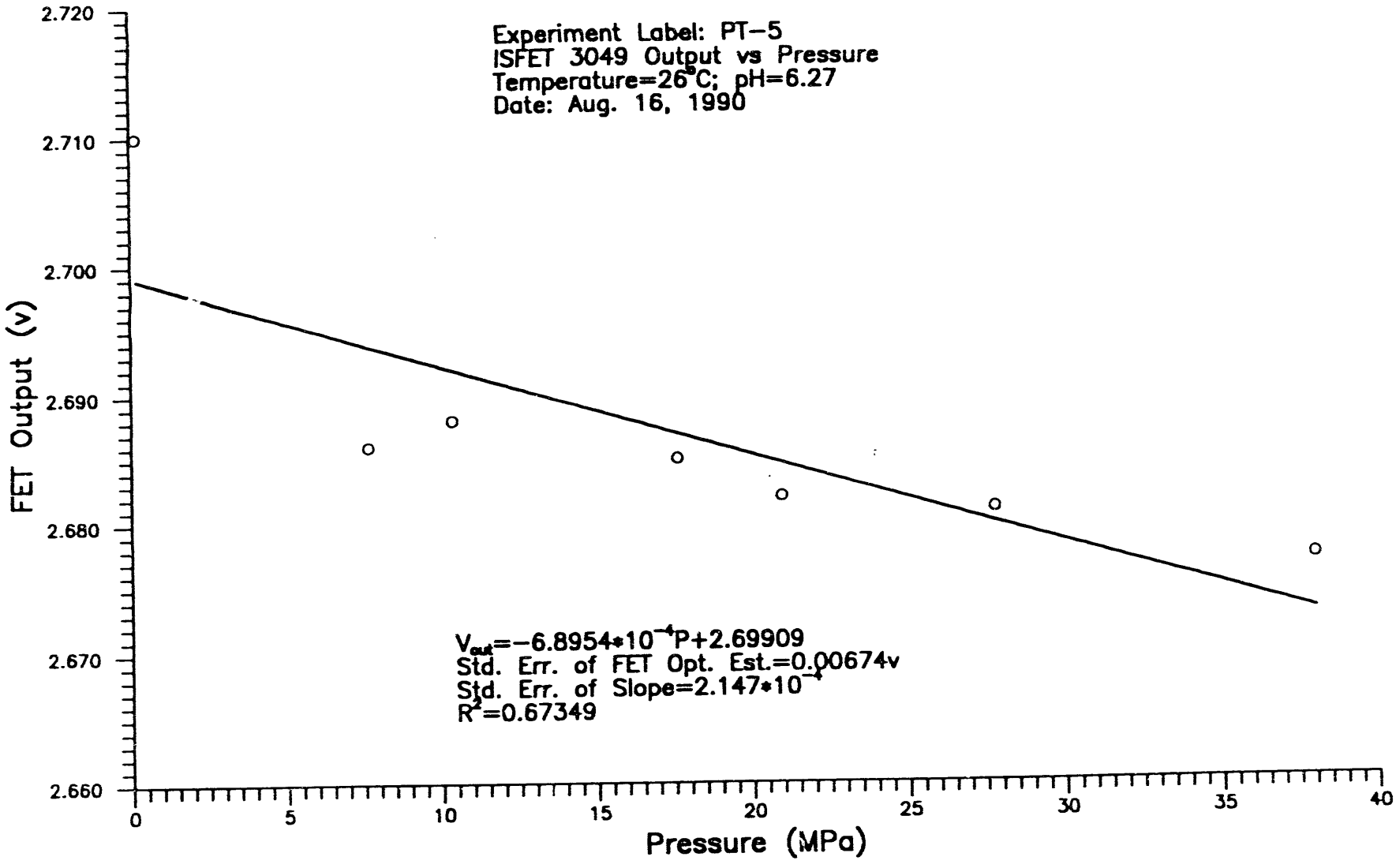

Figure 3.26 ISFET Output as a Function of Pressure at 26°C

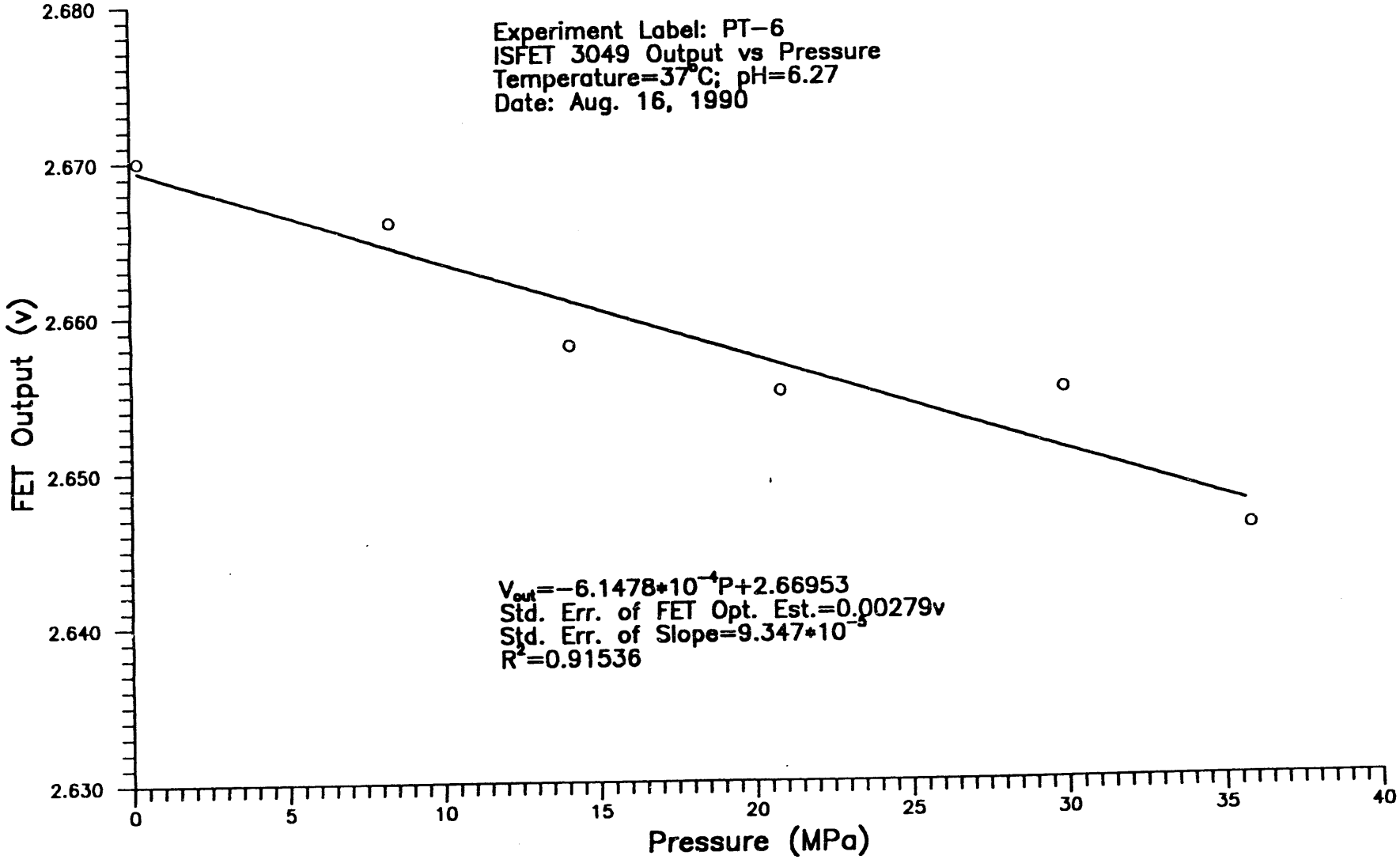

Figure 3.27 ISFET Output as a Function of Pressure at 37°C

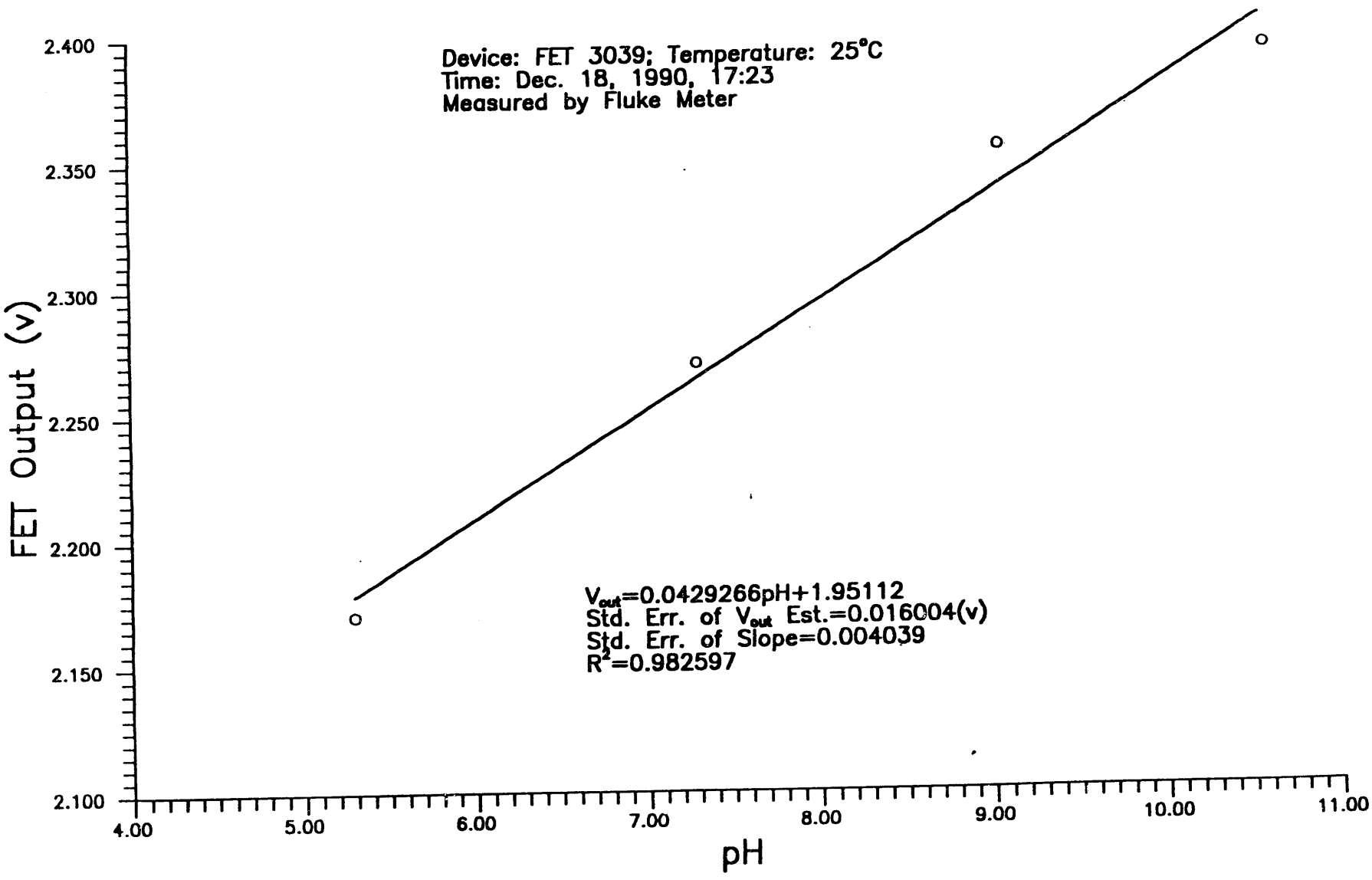

Figure 3.28 FET 3039 Output as a Function of pH Value

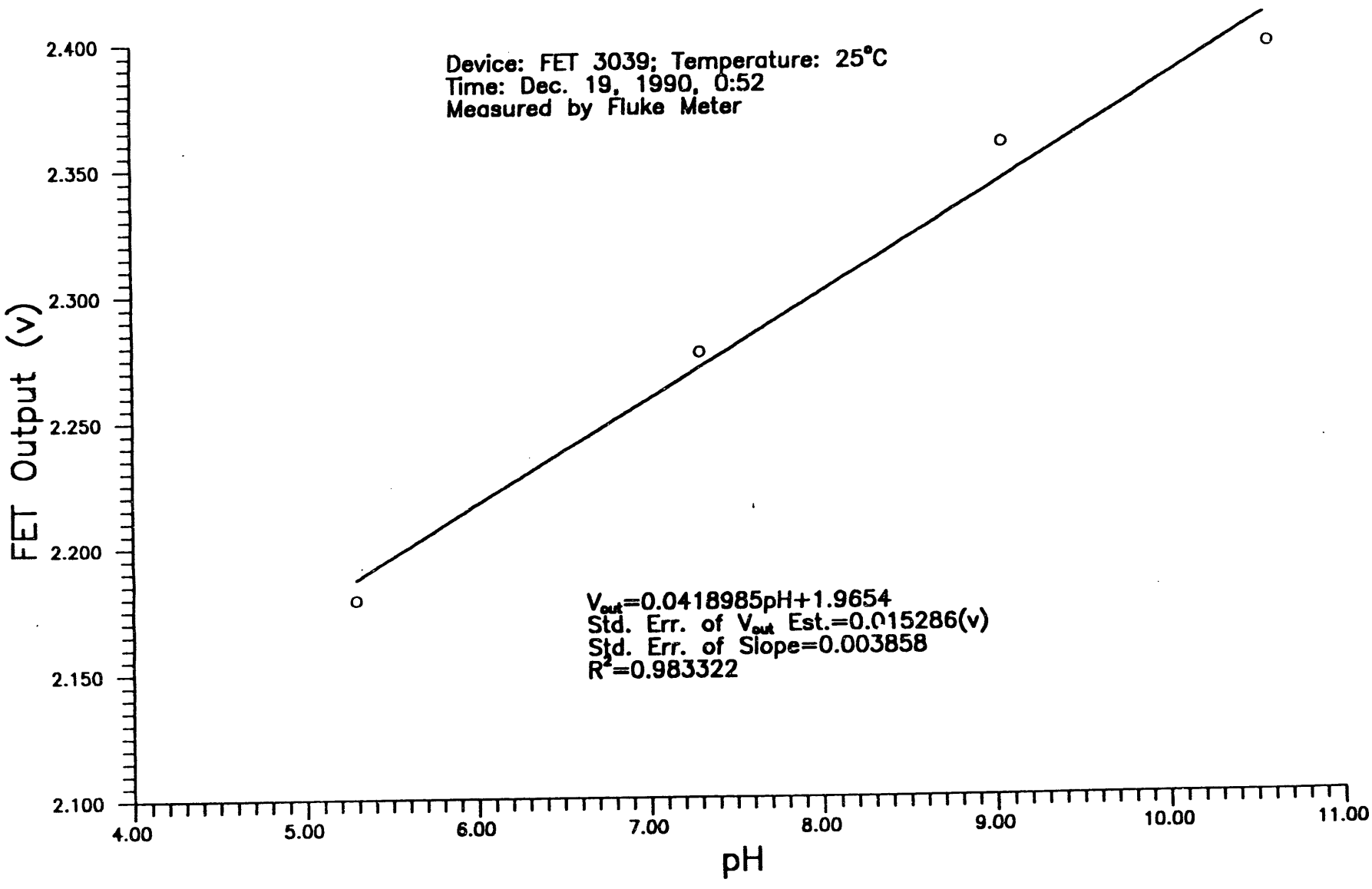

Figure 3.29 FET 3039 Output as a Function of pH Value

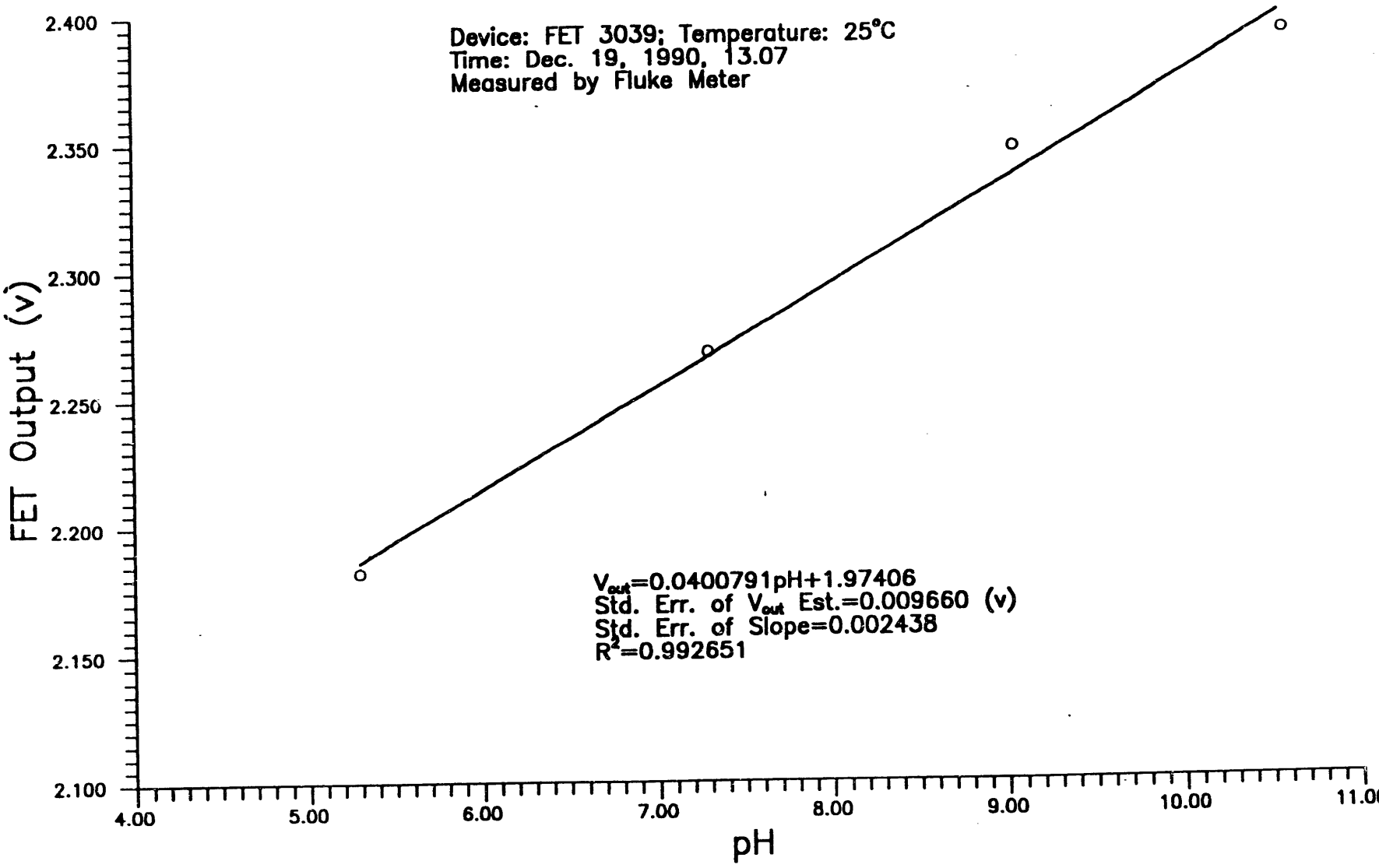

Figure 3.30 FET 3039 Output as a Function of pH Value

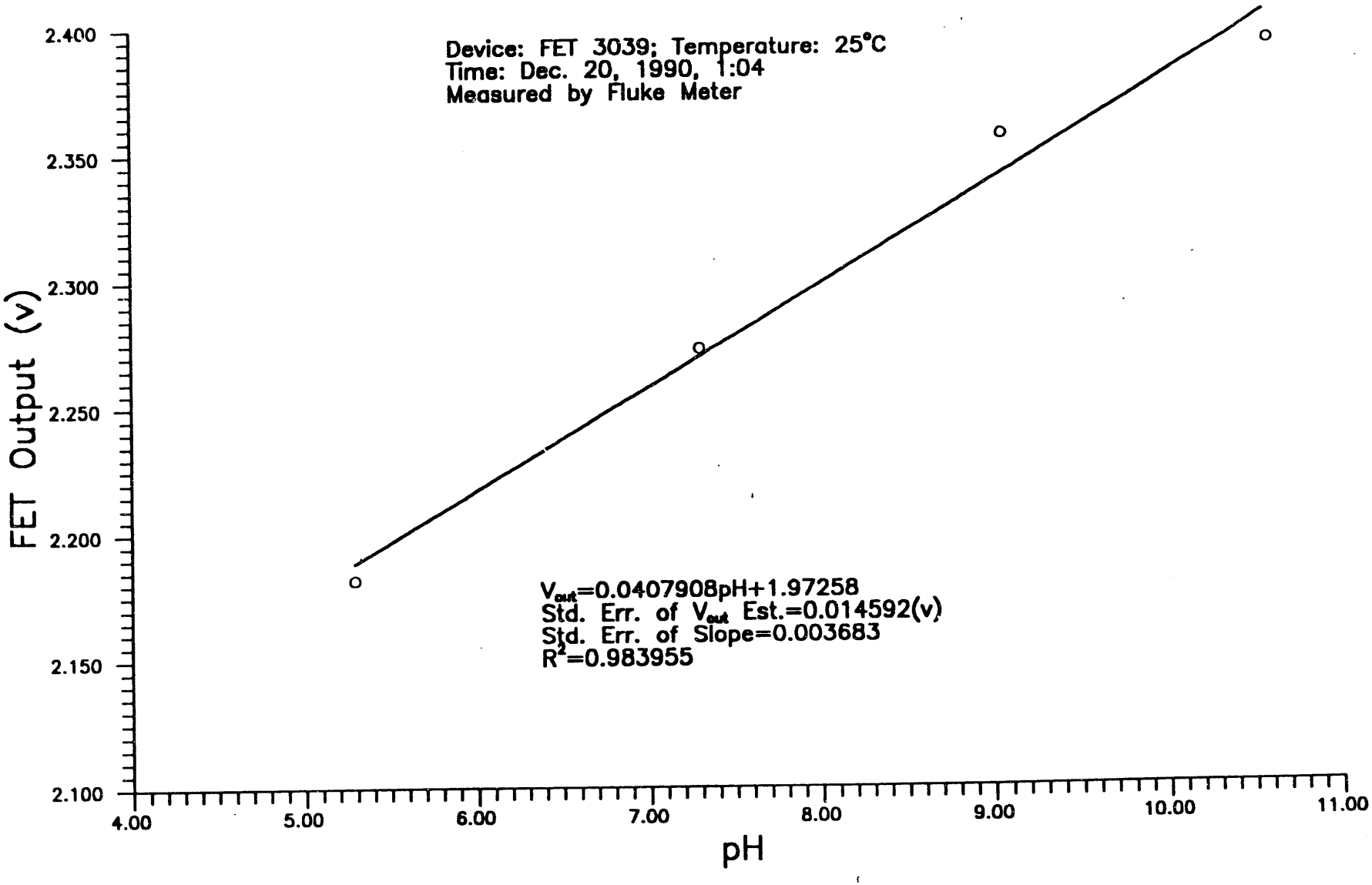

Figure 3.31. FET 3039 Output as a Function of pH Value

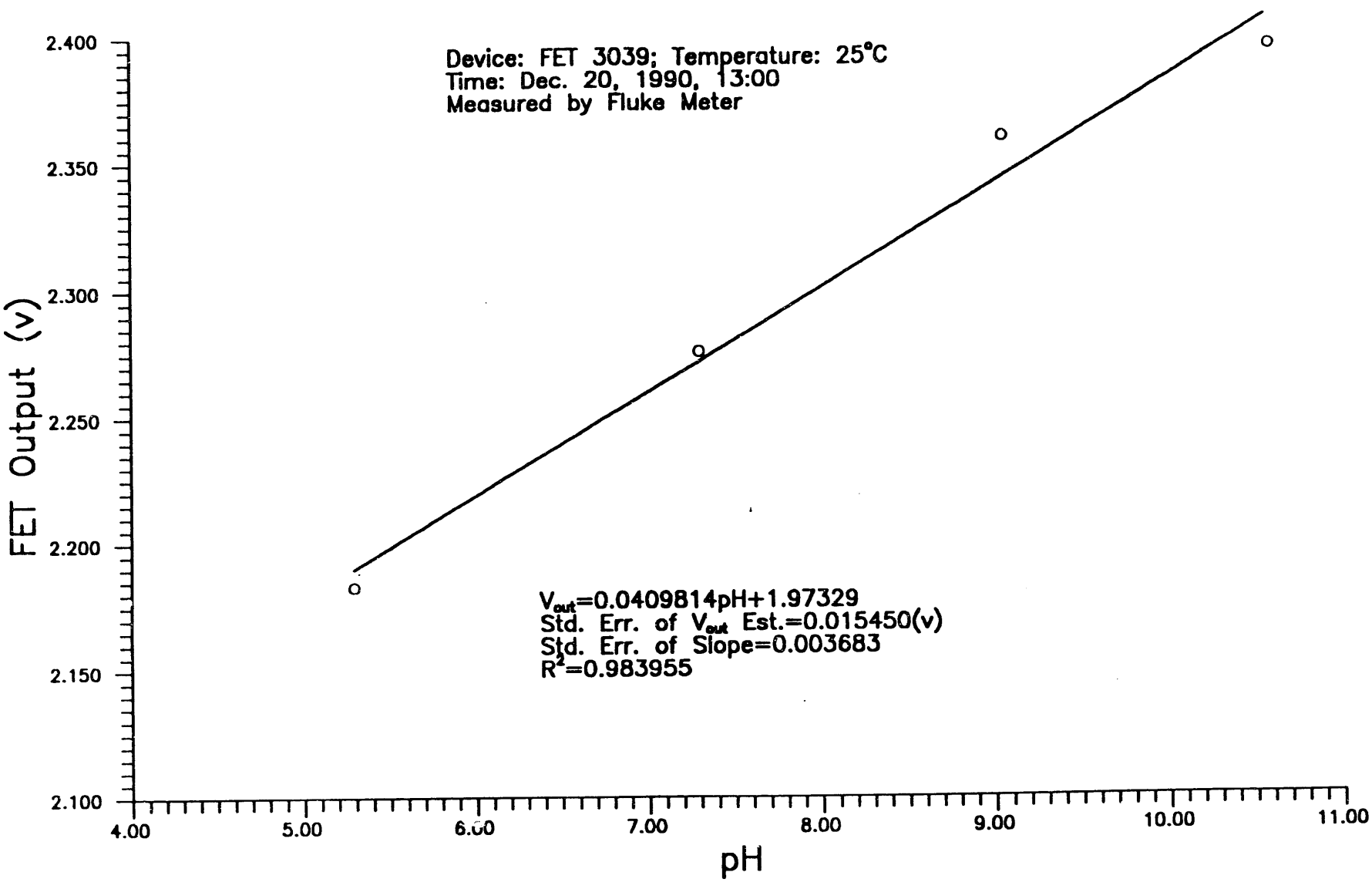

Figure 3.32 FET 3039 Output as a Function of pH Value

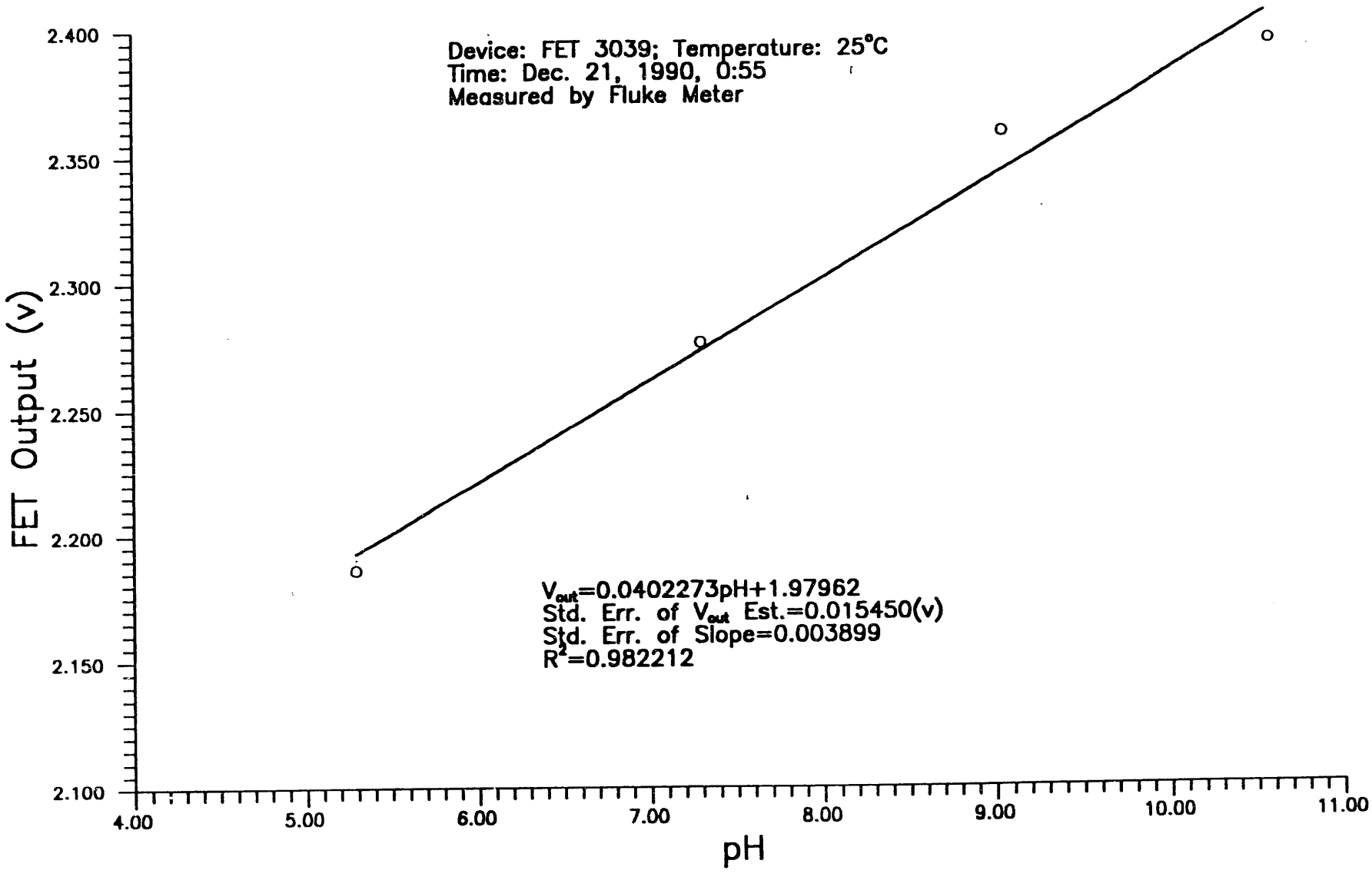

Figure 3.33. FET 3039 Output as a Function of pH Value

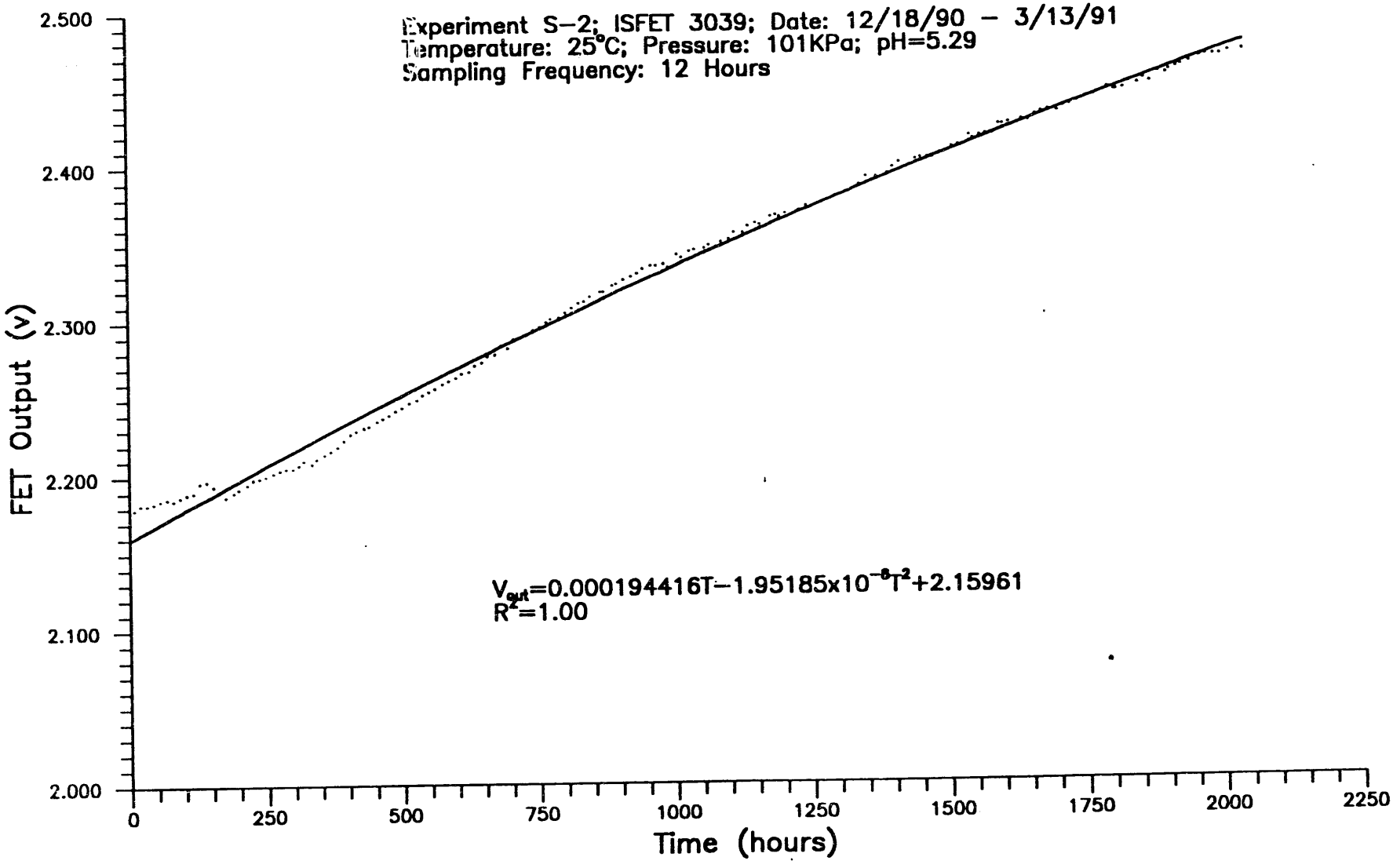

Figure 3.34 Stability Test of ISFET 3039 in pH 5.29 Buffered Solution

REFERENCES:

1. Benson, J., "New technology in pH analysis", *American Laboratory*, pp. 60-62, (March 1988).
2. Alean-Kirkpatrick, P. and Hertz, J. "An ion-selective field effect transistor for in-Situ pH monitoring of wet deposition" *Intern. J.Environ. Anal. Chem.*, **37**. pp. 149-159, (1989).
3. Knauss, K. G., Wolery, T. J. and Jackson, K. J., "A new approach to measuring pH in brines and other concentrated electrolytes". *Geochimica et Cosmochimica Acta*. **54**, pp. 1519-1523, (1990).
4. Baxter, R. D., Phelan. D. M., Clack, P. J. and Taylor, R. M.,"R&D fabrication and testing of pH and CO_2 sensors for geothermal brines", Leeds & Northrup Company, North Wales, PA., (Mar. 1987).
5. Bergveld, P., *IEEE Trans.* **BME-17**, pp. 70, (1970).
6. Matsuo, T., Esashi, M., and Iinuma, K., *Digest of joint meeting of Tohoku Sections of IEEEJ*, (Oct. 1971).
7. Bergveld, P., *IEEE Trans.* **BME-19**, pp. 342, (1972).
8. Matsuo, T., and Wise, K. D., *IEEE Trans.* **BEM-21**, pp. 485, (1974).
9. Freiser, H., "Ion-selective electrodes in analytical chemistry", **2** *Plenum Press*, New York and London, (1981).
10. Zemel, J. N., *Anal. Chem.* **47**, pp. 255A, (1975).
11. Moss, S. D., Janata, J., and Johnson, C. C., *Anal. Chem.* **47**, pp. 2238, (1975).
12. Revesz, A. G., *Thin Solid Films*, **41**, L43, (1977).
13. Buck, R. P., and Hackleman, D. E., *Anal. Chem.* **49**, pp. 2315, (1977).
14. Morf, W. E., Oggenfuss, P., Simon, W., "New developments and consequences of the theory of ion-selective membranes" *4th Symposium on Ion-Selective*

Electrodes. Mátrafüred, (1984).

15. Janata, J., "Chemically sensitive field effect transistors: their application in analytical and physical chemistry" *4th Symposium on Ion-Selective Electrodes*. Mátrafüred, (1984).
16. Van Der Schoot, B. H. and Bergveld, P., "The pH-static enzyme sensor" *Analytica Chimica Acta*, **199**, pp. 157-160, (1987).
17. Sibbald, A., Covington, A. K. and Carter, R. F., "Online patient-monitoring system for the simultaneous analysis of blood K^+, Ca^{2+}, Na^+ and pH using a quadruple-function CHEMFET integrated-circuit sensor" *Medical & Biological Engineering & Computing*, pp. 329-338, (July 1985).
18. Sibbald, A., Whalley, P. D. and Covington, A. K., "A miniature flow-through cell with a four-function CHEMFET integrated circuit for simultaneous measurements of potassium, hydrogen, calcium and sodium ions", *Analytica Chemica Acta.*, **159**, pp. 47-62, (1984).
19. Sibbald, A., "A chemical sensitive integrated circuit: the operational transducer", *Sensors and Actuators*, **7**, pp. 23-38, (1985).
20. Bousse, L., De Rooij, N. F. and Bergveld, P., "Operation of chemical sensitive field-effect sensors as a function of the insulator-electrolyte interface", *IEEE Transaction on Electron Devices*, **ED-30, No. 10**. (Oct. 1983).
21. Li, Z. K., Reijn, J. M. and Janata, J., "Fluctuation phenomena studies in chemically sensitive field effect transistors", *J.Electrochem. Soc.* (Mar. 1985).
22. Cakrt, M., "Optimization of experimental methods for determination of selectivity coefficients of known-addition techniques", *4th Symposium on Ion-selective Electrodes*, Mátrafüred, (1984).
23. Van Der Spiegel, J., Lauks, I., Chan, P., Babic, D., "The extended gate

chemically sensitive field effect transistor as malt-species microprobe", *Sensors & Actuators*, **4**, pp. 292, (1983).

24. Janata, J., "Chemical selectivity of field effect transistors", *Analytical Proceedings*, pp. 326-328, (Nov. 1987).
25. Braun, R. D.,"Introduction to instrumental analysis", pp. 697-720, McGraw-Hill Book Company, (1987).
26. Mann, L. Jr. "Applied engineering statistics for practicing engineers", pp. 113-134, Branes & Noble, Inc., New York, (1970).
27. Volk, W., "Applied statistics for engineers", pp. 268, McGraw-Hill Book Co., (1969).

For a Thesis

Chen, Jie, University of Southwestern Louisiana, 1991
Master of Science, Summer 1991
Major: Physics
Title of Thesis: Ion Sensitive Field Effect Transistors Applied to the Measurement of the pH of Brines
Thesis Directed by Dr John R. Meriwether
Pages in Thesis, 84; Words in Abstract, 125.

Abstract: In this research, Ion Sensitive Field Effect Transistors were used as the pH probes for brine solutions. A silver-silver chloride coated wire electrode was used as the reference electrode. Several pH values of buffer solutions containing sodium chloride were prepared as calibration and test solutions. The high pressure and high temperature conditions found in geothermal/geopressured reservoirs were maintained on the test solutions by a temperature and pressure control system. Measurements of ISFET's output, V_{out}, as a function of pH, temperature, and pressure were performed. Linear relationships between V_{out} and pH, V_{out} and temperature, and V_{out} and pressure were obtained and studied. The ISFETs were stable and reliable up to at least 40 MPa, but generally failed at temperatures in excess of about 60°C.

Biographical Sketch

Jie Chen, born in Xiamen, China on May 1, 1964, obtained his B.S. degree in physics at Jilin University, China in July, 1985. Working as an assistant engineer with Xiamen Photo. Materials Co. Ltd. from August, 1985 to December, 1988, he was charged with the analysis of photographic particles using an electromicroscope. In the Spring of 1989, he began his graduate study at the University of Southwestern Louisiana, USA.. While studying at USL, he was first a graduate teaching assistant and then during the Summer of 1989 he became a research assistant for Dr. John R. Meriwether and Dr. Dean F. Keeley at the Acadiana Research Laboratory.

END

DATE
FILMED
2/22/93